

Evaluating the change in net CO₂ exchange caused by flooding a black spruce forest
through the creation of a hydroelectric reservoir

by

William Tianqi Xing

A Thesis Submitted in Partial Fulfillment of the Requirements for the Degree of B.Sc. in
Geography

Department of Geography
McGill University
Montréal (Québec) Canada

March 2020

© William Tianqi Xing

Table of Content

List of Figures	iii
List of Tables	vi
Abstract	vii
Chapter 1: Introduction	1
1.1 Study background	1
1.2 Research questions and study aims	2
1.3 Thesis format	3
Chapter 2: Literature Review	4
2.1 Carbon exchange in the boreal forest.....	4
2.2 Carbon exchange in flooded environment	5
2.3 Eddy covariance technique	6
2.4 Gap-filling strategies.....	8
Chapter 3: Methodology	10
3.1 Study site.....	10
3.1.1 Climate.....	11
3.1.2 Biogeography	11
3.2 Eddy covariance for flux measurement	11
3.3 Gap-filling strategy	12
3.3.1 Forest data.....	12
3.3.2 Reservoir data	12
Chapter 4: Result	14
4.1 Meteorological facts of two data sites	14
4.1.1 Temperature at the forest site.....	14
4.1.2 Temperature at the reservoir site.....	15
4.1.3 Wind characteristics	17
4.2 Net Ecosystem Exchange pattern in forest site.....	19

4.2.1	Diurnal and monthly NEE pattern	19
4.2.2	Annual NEE pattern	22
4.2.3	Cumulative pattern of NEE.....	24
4.3	CO ₂ flux pattern in reservoir site	25
4.3.1	Diurnal and monthly CO ₂ flux pattern.....	25
4.3.2	Annual cumulative CO ₂ flux pattern.....	30
4.4	Net Effect of the reservoir.....	31
Chapter 5: Discussion		34
5.1	Flux comparison.....	34
5.1.1	Forest NEE.....	34
5.1.2	Flooded site CO ₂ emission.....	35
5.2	Study limitations	35
Chapter 6: Conclusion		37
Reference List		39
Appendix: Links for used scripts in the study.....		43

List of Figures

Figure 1.1 Canada electricity generation by source, 2017. Figure retrieved from Natural Resources Canada, https://www.nrcan.gc.ca/science-data/data-analysis/energy-data-analysis/energy-facts/electricity-facts/20068	2
Figure 2.1 World Biome Map. Figure retrieved from webpage of Arizona State University https://askabiologist.asu.edu/explore/biomes	4
Figure 2.2 Eddy covariance tower. Figure retrieved from https://www.n.ethz.ch/~sewolf/personal/projects.html	8
Figure 3.1 Landmass classified figure of Eastmain-1 reservoir and surrounding boreal territory	10
Figure 3.2 Empirical approach gap-filling algorithm, Lasslop et al., 2010	13
Figure 4.1 Daily averaged air and soil temperature at the forest site; Ta (°C) air temperature, Ts (°C) soil (ground) temperature from March 28 th , 2007 to September 23 rd , 2012	15
Figure 4.2 Daily averaged air temperature (°C) of the reservoir site for 2008, 2009, 2011 and 2012.....	16
Figure 4.3 Wind rose of Eastmain-1 reservoir wind direction and intensity (speed), annually.....	18
Figure 4.4a Diurnal NEE ($\mu\text{mol m}^{-2} \text{s}^{-1}$) variation at the forest site in 2007	20

Figure 4.4b Diurnal NEE ($\mu\text{mol m}^{-2} \text{s}^{-1}$) variation at the forest site in 2008	21
Figure 4.4c Diurnal NEE ($\mu\text{mol m}^{-2} \text{s}^{-1}$) variation at the forest site in 2009.....	21
Figure 4.4d Diurnal NEE ($\mu\text{mol m}^{-2} \text{s}^{-1}$) variation at the forest site in 2010	21
Figure 4.4e Diurnal NEE ($\mu\text{mol m}^{-2} \text{s}^{-1}$) variation at the forest site in 2011	22
Figure 4.4f Diurnal NEE ($\mu\text{mol m}^{-2} \text{s}^{-1}$) variation at the forest site in 2012	22
Figure 4.5 Relationship between air and soil surface temperature ($^{\circ}\text{C}$) and NEE ($\text{g C m}^{-2}\text{d}^{-1}$) at the forest site	23
Figure 4.6 Daily sum of the 30-minute averaged PPFD at the forest site for six study years	24
Figure 4.7 Annual cumulative ER, GEP and NEE at the forest site for 2008-2012	25
Figure 4.8a Diurnal CO_2 flux at the flooded site in 2008	26
Figure 4.8b Diurnal CO_2 flux at the flooded site in 2009.....	26
Figure 4.8c Diurnal CO_2 flux at the flooded site in 2011	27
Figure 4.8d Diurnal CO_2 flux at the flooded site in 2012.....	27
Figure 4.9 Daily averaged CO_2 flux at the flooded site for 2008 2009 2011 and 2012....	29

Figure 4.10 Daily averaged CO ₂ flux at the flooded site for 2008 2009 2011 and 2012 (combined)	30
Figure 4.11 Cumulative CO ₂ flux at the flooded site. The portion of 2012 indicated by the green line is the estimated flux found by averaging the previous three years	31
Figure 4.12a Net effect of carbon emission in 2008	32
Figure 4.12b Net effect of carbon emission in 2009	32
Figure 4.12c Net effect of carbon emission in 2011	33
Figure 4.12d Net effect of carbon emission in 2012, the dotted line is the estimated flux for 2012 averaged by the previous three years	33

List of Tables

Table 4.1 Monthly mean air and soil surface temperature of the forest site	14
Table 4.2 Extrema and means of 30-min recorded air temperature at the reservoir site ...	16
Table 4.3 Gap percentage of wind speed/direction data.....	17
Table 4.4 Monthly mean NEE of the forest site	19
Table 4.5 Annual growing seasons of the forest site	20
Table 4.6 Annual cumulative flux of the forest site	25
Table 4.7 Annual cumulative flux of the flooded site	30
Table 4.8 Net carbon flux effect of the reservoir creation.....	32
Table 5.1 NEE comparison between the present study and three studies taken in Canadian old Black Spruce forests	34
Table 5.2 Comparison between the present study and northern hydroelectric reservoir CO ₂ emission	35

Abstract

The research evaluates the magnitude and direction of carbon exchange resulting from the impoundment of a boreal forest for hydroelectric purposes and determines the net effect of the impoundment. NEE was measured by the eddy covariance technique from March 29th, 2007 to September 24th, 2012 in an unaffected mature black spruce forest and a flooded forest within the Eastmain-1 reservoir, both located in the James Bay region of Quebec, Canada. The forest site acts as a pre-flooded analogue site to the newly impounded reservoir. Flux result showed that the intact forest is a net carbon sink (-21 to -103 g C m⁻²yr⁻¹) whereas the flooded site is a constant CO₂ emitter (98 to 171 g C m⁻²yr⁻¹). Adding the post-flood emission to the loss of sink reveals that the net reservoir effect ranges from an annual emission of 181 to 242 g C m⁻²yr⁻¹. Flooding a boreal forest results in a net increase of carbon emission to the atmosphere.

1. INTRODUCTION

1.1 Study background

Research on the effect of hydroelectric reservoir on carbon exchange has been conducted for years and in distinctive approaches. Field research has ranged from short term studies on small impoundments to long term effects of extensive reservoirs. The total extent of the reservoirs worldwide is significantly large. An estimated 16.7 million reservoirs larger than 0.01 ha worldwide increases the world terrestrial water surface by at least 305,000 km² (Lehner, 2011). At the very largest scales, Chao (1994, 1995) reported that globally, the impoundment of water in reservoirs has reduced sea levels by 3 cm (Rosenberg et al., 1997). Research at larger scales has begun to lead to new views about the spatial extent and longevity of the environmental and social effects of such projects, and cumulative effects on a global basis. It has been widely accepted that dams and reservoirs, especially large ones, can induce substantial effects to both human societies exemplified by resident resettlement (for example Wilmsen et al., 2011; Jackson and Sleigh, 2000), and changes in water and food security (Umehara et al., 2019); and the natural environment with a myriad of outcomes such as changes of fish migration pattern (Xu et al., 2017), and release of anthropogenic greenhouse gases including carbon dioxide (Louis et al., 2000) which is the main interest of this thesis to study and discuss.

It is generally accepted that the flooding and transformation of a terrestrial ecosystem to a lake or reservoir, either by natural processes or human activities, can result in a loss of a sink of atmospheric carbon dioxide (Louis et al., 2000; Tremblay et al. 2004). Following the flooding of a former terrestrial ecosystem, terrestrial plants die and are no longer able to fix atmospheric carbon dioxide by photosynthesis. Furthermore, plant tissues are then decomposed by aquatic microorganisms and bacteria, with organic carbon in plant tissues subsequently converted into carbon dioxide and released into the atmosphere; thus, turning a natural sink of carbon to a source.

Much of the research to date has been in temperate and tropical reservoirs. Canada has

a very large area of boreal ecosystems with ample freshwater resources. In 2017, hydropower provided about 60% of the electricity supply in Canada and even occupied 95% of the total electricity production in Quebec (Figure. 1.1, Natural Resources Canada). Hydroelectric plants are mainly located within an ecosystem characterized as black spruce boreal forest. The effects of a hydroelectric reservoirs on the natural environment are likely to increase in Quebec as electricity demand grows and more impoundments could be built. Thus, it is a great interest to study the effects on carbon dioxide that these young reservoirs could induce.

GENERATION BY SOURCE, 2017

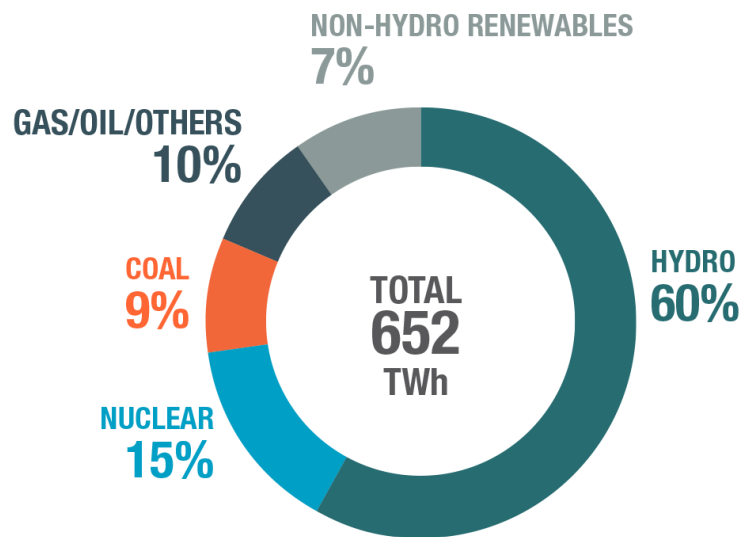


Figure 1.1 Canada electricity generation by source, 2017. Figure retrieved from Natural Resources Canada, <https://www.nrcan.gc.ca/science-data/data-analysis/energy-data-analysis/energy-facts/electricity-facts/20068>

1.2 Research questions and study aims

The overarching question that this thesis asks is: “What is the net effect that the creation of a boreal hydroelectric reservoir has on the net exchange of CO₂?” The hypothesis is that creating a hydroelectric reservoir by flooding a boreal forest ecosystem

will increase the net emission of CO₂ and change the ecosystem from a net sink to a net source of carbon. The magnitude of the change is also of interest.

In this research we use tower-based eddy covariance system to quantify the continuous CO₂ exchange over a flooded site and a pre-flooded site around a boreal hydroelectric reservoir. By comparing the continuous CO₂ emissions, we are able to quantify the net effect of the flooding.

1.3 Thesis format

This thesis consists of six chapters including this introductory chapter. Chapter 2 provides a review of the research conducted to date on hydroelectric reservoir creation in northern environments with emphasis on CO₂ emissions. Chapter 2 also provides a review of research on the measurement techniques as well as gap-filling strategies. A methodology chapter follows this review and describes the setting of the research. The carbon exchange results of the reservoir and an analogue boreal black spruce forest are presented in Chapter 4. The direction and the magnitude of the net effect is then presented at the end of Chapter 4. Comparative studies of carbon exchange in boreal reservoirs are presented in Chapter 5. The results are compared with the current study. The thesis culminates in Chapter 6 where a summary of the research is presented.

2. LITERATURE REVIEW

2.1 Carbon exchange in the boreal forest

Boreal forests occupy 22% of the global forested area, or about 1.2×10^7 km², nearly half of Canada's territory is covered by boreal forest (Iremonger et al. 1997, Schlesinger 2013). The boreal forest ecotone extends in the Northern Hemisphere from the mid-latitudes to the subarctic in a broad swath that encompasses large parts of Russia, Scandinavian countries and Canada (Figure 2.1). Carbon in the boreal forest is unevenly distributed: nearly half of global soil carbon is stored in the boreal forest but biomass above the ground only occupies 13% of global carbon biomass, whereas the rest is stored in the soil. The landscape of boreal biomes is heterogeneous with varying stand ages and land cover types (Dunn et al., 2009).

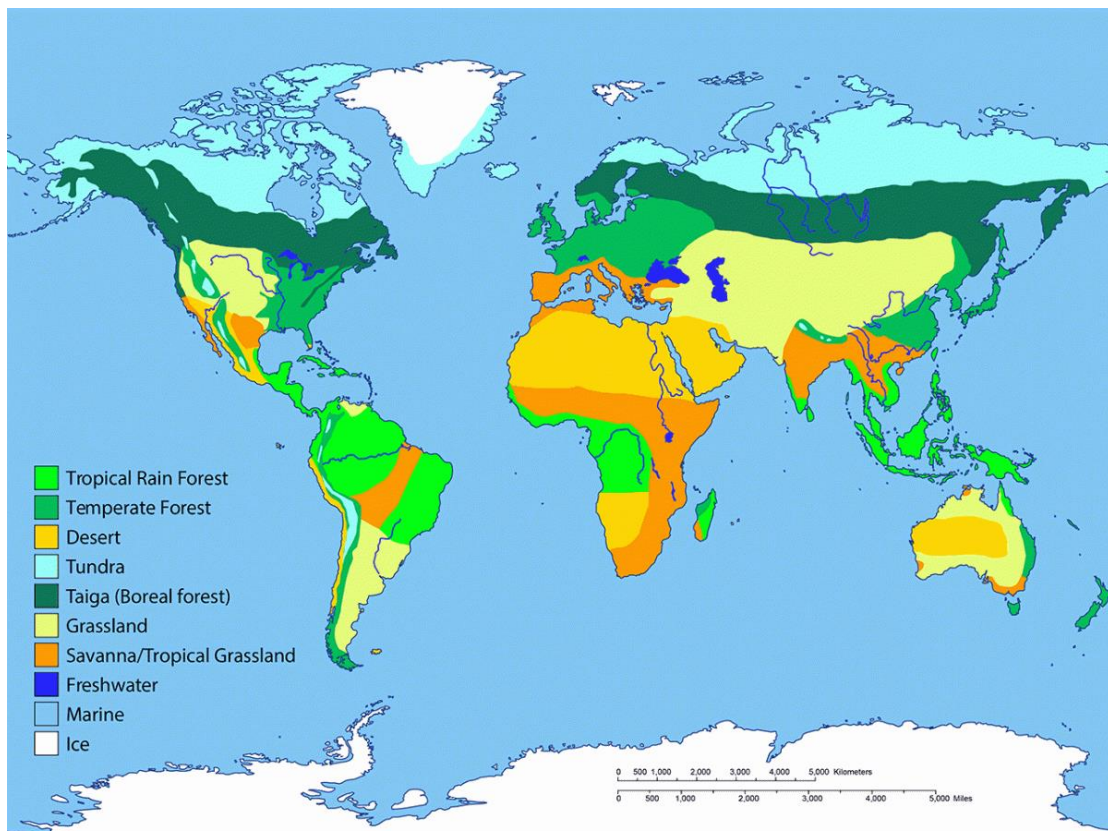


Figure 2.1 World Biome Map. Figure retrieved from webpage of Arizona State University <https://askabiologist.asu.edu/explore/biomes>

Dunn et al. (2007) recorded a 10-year CO₂ flux (1994-2004) record in a 160-year old boreal forest in Manitoba. They concluded that ecosystem carbon exchange responded strongly to air temperature, moisture status and evapotranspiration. However, they found no clear correlation between longer growing seasons and net carbon uptake, which was likely caused by offsetting increases in ecosystem respiration.

More recently, Dunn et al. (2009) observed that in boreal forest peatland, soil temperatures were positively correlated with the peatland respiration rates, and drainage status of soil also play a role. They concluded that the soil respiration rate is driven by soil temperature and enhanced by a lower water table. Strachan et al. (2015) also concluded that the inter-annual variability of NEE (especially for summer time photosynthesis rate) in boreal peatland is primarily linked to change in water table depth.

McMillan et al. (2008) measured the CO₂ exchange at six Canadian boreal forest sites to determine how the age of the forest affects the response to interannual temperature and precipitation variation. They concluded that the major cause of interannual CO₂ exchange variation at the landscape scale is due to an earlier launch of photosynthesis in older evergreen trees when there is a warmer spring.

2.2 Carbon exchange in flooded environment

Previous study of a reservoir in North America (Tadonl  k   et al., 2011) revealed drivers of carbon exchange in flooded environment, such as water temperature, dissolved organic matter and bacterial production. Using floating chamber measurements, Tremblay et al. (2004) revealed that the age of a reservoir is an important parameter to its carbon exchange. Reservoirs older than ten years are comparable to natural lakes or rivers in terms of gross CO₂ fluxes, whereas younger reservoirs emit higher amounts of CO₂ for the first 6 to 8 years.

The model “Flooded Forest Denitrification Decomposition” was used to simulate CO₂ exchange from boreal forest landscapes. Kim et al. (2016) used CO₂ measurements from

the Eastmain-1 reservoir in northern Quebec to validate the model and simulate future CO₂ exchange in 100 years. They concluded that vegetations, soil types and decomposable soil carbon in flooded ecosystems were important determinants of reservoir CO₂ emission. The study emphasized the significance of spatial and temporal variation in CO₂ flux from a boreal reservoir.

Intra-annual variation of CO₂ emission is highly affected by ice melt, air temperature and wind speed (Rosa et al., 2002). Coldwater has a smaller solubility and is not able to hold much CO₂. In spring, the first day of ice melt can be a CO₂ emission peak.

2.3 Eddy covariance technique

Traditional flux measurement techniques might lead to high biases and artifacts. Two typical examples of traditional flux measurement techniques are leaf cuvette and carbon chamber system. For leaf cuvette, measurements are highly limited by the number of cuvettes that can be set up and the timespan that a plant canopy is presented for measurement (Baldocchi, 2003). Similarly, the carbon chamber technique can only provide a relatively small flux measurement extent, which does not fit the scale of the boreal forest very well. Furthermore, a chamber creates an artificial environment with perturbation of local temperature, pressure, moisture and wind fluxes (Livingston et al., 1995).

Eddy covariance is now the standard technique for measurement of CO₂ fluxes at the ecosystem scale. It is essentially an atmospheric measurement technique that measures vertical turbulent fluxes within the atmospheric boundary layer. The instrument has two major parts: an anemometer measuring instantaneous wind speed and a high-frequency gas analyzer measuring CO₂ concentration (Figure 2.2). With two quantities measured, a flux of C (F_c in $\mu\text{mol m}^{-2}\text{s}^{-1}$) in covariance can be calculated as:

$$F_c = \overline{\left(\rho_a \cdot w' \left(\frac{\rho_c}{\rho_a} \right)' \right)} \quad (1)$$

where w is the vertical wind speed in terms of ms^{-1} , ρ_a is the air density, ρ_c is the CO₂

density, and ρ_c/ρ_a is the mixing ratio of CO₂ in the atmosphere. The overbar is a time average (typically 30-minutes) and the prime indicates an instantaneous departure from the average. This equation is typically simplified as:

$$F_c = \overline{w'\rho_c'} \quad (2)$$

A great advantage of eddy covariance over traditional flux measurement techniques is data continuity. Eddy covariance can provide continuous flux data throughout the year (Baldocchi, 2003). Data from eddy covariance is reported half-hourly with an objective to collect data 24 hours a day and 365 days a year (Falge et al. 2001). With the resulting dataset, flux density at different temporal scales (daily, monthly and annually) can be calculated straightforward. Eddy covariance should be set up over a flat and homogeneous surface to enhance the stability of flux measurement. However, technical and power failure, as well as extreme weather conditions, can lead to malfunction of eddy covariance and subsequently create data gaps. Useful data coverage can typically occupy 65% of a year (Falge et al., 2001); thus, further data processing may need a gap-filling procedure.

In this research, eddy covariance is specifically used to measure the net ecosystem exchange (NEE) of CO₂, which is defined as the net difference between the uptake of CO₂ mainly by photosynthesis (gross ecosystem production (GEP)) and the release of CO₂ by ecosystem respiration (ER).

$$NEE = ER - GEP \quad (3)$$

Therefore, by convention, negative values of NEE represent an uptake as GEP is larger than ER.

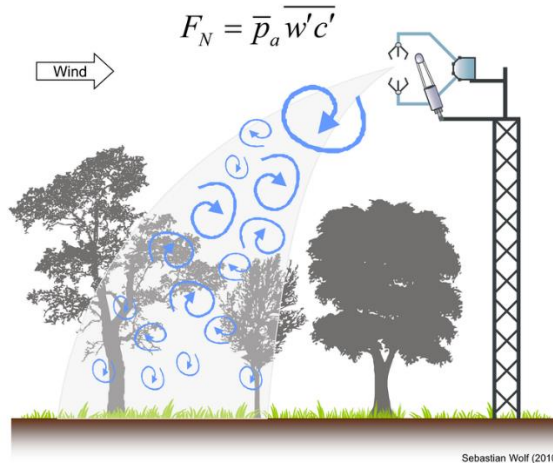


Figure 2.2 Eddy covariance tower. Figure retrieved from <https://www.n.ethz.ch/~sewolf/personal/projects.html>

2.4 Gap-filling strategies

Eddy covariance data can be affected by technical failure or damage from extreme weather conditions, and recording gaps could be generated, making the data set not perfectly continuous. Falge et al. (2001) made a detailed study of gap filling strategies. The most appropriate method of gap-filling may be influenced by the characteristic uniqueness at a flux tower site and the end-use of the flux data. There is no standard widely accepted gap-filling method, however several strategies can be performed. For example, some studies have used mean diurnal variation to estimate annual and seasonal sum of NEE flux for forests (Greco and Baldocchi, 1996); while other studies adopted a variation of light response function to estimate the flux of NEE in data gaps (Granier et al. 2000). It is also feasible to use two types of flux measurement techniques-for example eddy covariance and carbon chamber-at the same time to reduce the occurrence of gaps (Law et al. 1999a, 1999b). But it is still a mystery whether there exists a gap-filling method that can be applied universally.

For small gaps, typically 2-3 half-hourly missing data, interpolation can be simply applied. Thus, interpolation is usually adopted as an optional data pre-treatment before filling larger gaps. For larger data gaps, there are specialized algorithms to follow.

Specifically, Falge et al. (2001) mainly discussed mean diurnal variation where the missing data is replaced by the mean of that period based on adjacent days; and semi-empirical methods which can be further categorized as look-up tables and non-linear regression. Look-up table is created based on the averaged behaviour of a particular condition within a defined time span (e.g. monthly, seasonally); it can be regarded as a reference to help fill the missing data. Non-linear regression establishes a regression relationship between flux and associated controlling factors for each site and period of the year, where the resulting regression formula would be used to fill the data gaps. Falge et al. (2001) recommended the use of semi-empirical methods if possible because these methods preserve the response of NEE flux to primary meteorological conditions such as a variation on temperature and PPFD.

3. METHODOLOGY

3.1 Study site

The study site of this research is at the Eastmain-1 reservoir, located within the James Bay region of Quebec with a surface area of 603 km² (Figure 3.1). It is a typical boreal ecoregion about 800 km north of Montreal. Specifically, two eddy covariance towers were constructed for data collection. One was located in a black spruce forest site (52°06'16" N, 76°11'48") and represented the pre-flooded ecosystem (near the left edge of the figure), and the other was located on the edge of an island (central-left) in the Eastmain-1 reservoir (52°07'29" N, 75°55'47") and represented the flooded black spruce ecosystem.

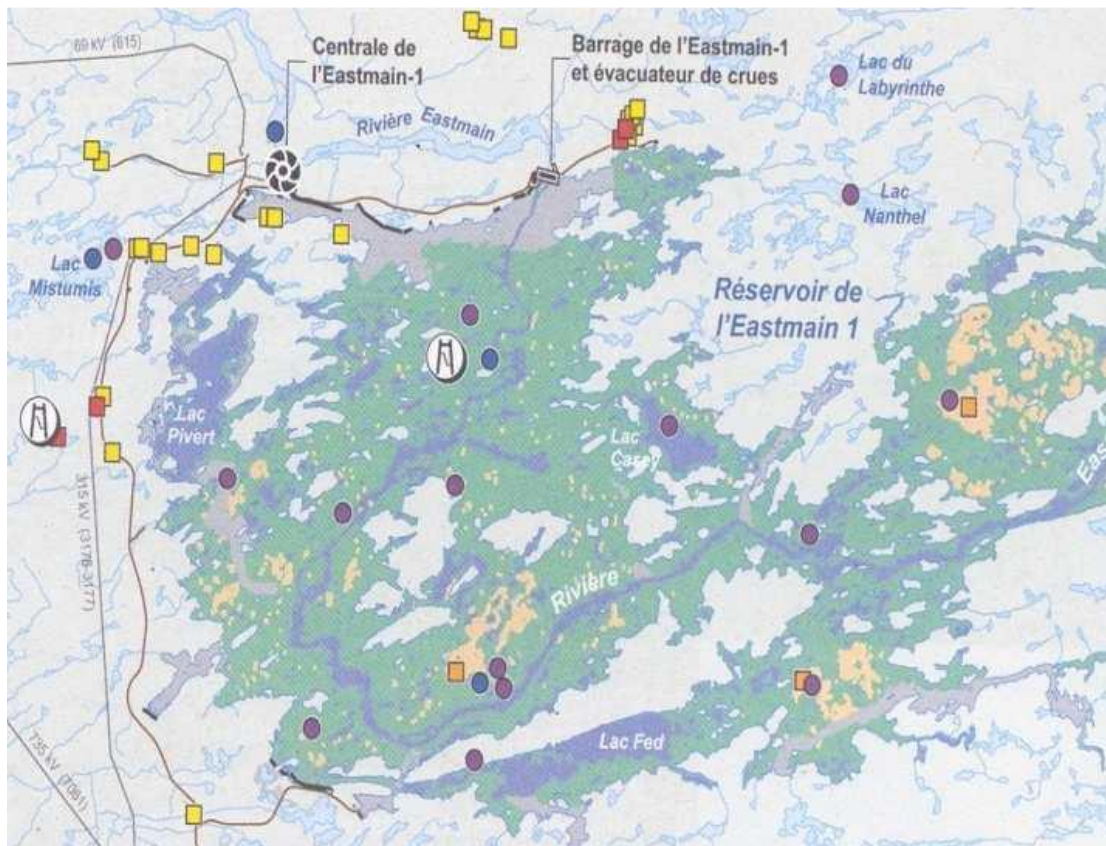


Figure 3.1 Landmass classified figure of Eastmain-1 reservoir and surrounding boreal territory (Lemieux, 2010)

3.1.1 Climate

The Eastmain-1 reservoir is typically within the boreal forest biome with harsh and long winters, and short summers. The reservoir is covered with ice about 180 days per year. Runoff is strongly seasonal, with peak flow in late spring when the ice starts to melt (May and June) and the lowest flow in late winter due to frozen of ice. Mean annual temperature is close to 0, with a mean annual precipitation between 700 mm and 900 mm (Strachan et al., 2016; Tremblay et al., 2020).

Climate data of the study site were collected by two eddy covariance towers. Dataset of the forest site covered from March 28th, 2007 to September 24th, 2012. Key gap-filled climatic data includes air temperature, soil surface temperature, photosynthetic photon flux density, ecosystem respiration, gross ecosystem production, and the wind direction and the wind speed at the reservoir site.

3.1.2 Biogeography

The pre-flooded landscape is composed by a diversity of terrestrial and aquatic ecosystems. Specifically, 182 km² of the pre-flooded landscape (30%) consisted of mature forest (91% coniferous and 9% deciduous), 114 km² of the pre-flooded landscape (19%) represented by burned (predominantly coniferous) forest, 46 km² (8%) represented by non-forest soil and 111 km² (18%) represented by wetlands (1% fen, 77% bog and 22% swamp/marsh). The remaining 150 km² (25%) is represented by lakes and rivers (Teodoru et al., 2012).

3.2 Eddy covariance for flux measurement

Eddy covariance was used to measure the NEE from the boreal forest at the study site. The primary measurement components included a sonic anemometer (CSAT3, Campbell Scientific, Edmonton), a fine-wire thermocouple and an open-path infrared gas analyzer (LI7500, Li-Cor, Lincoln, NE).

The flux measurement of forest site began on March 28th, 2007 and ended on September 24th, 2012, covering a time span of 2007 days. The ending day of the flooded site is three days earlier than the forest site, on September 21st, 2012. All data were recorded using a data logger with a frequency of 10 Hz, and 30-minute averaged fluxes were computed and recorded.

Once the flux measurement is available, ER is derived from a soil T model and GEP from a PPFD model. For a non-terrestrial system such as the flooded site in current study, an assumption is made that there is no GEP and that the tower-recorded NEE is entirely ER.

3.3 Gap-filling strategies

Because there are two sites for flux measurement with different environmental conditions, the gap-filling strategies were applied separately to two datasets.

3.3.1 Forest data

NEE data was divided based on growing seasons, non-growing seasons, daytime and nighttime. Each gap less than four half hours in length was auto-filled by linear interpolation.

For longer gaps outside of growing seasons, gaps in ER were filled using an NEE-soil temperature relationship developed for nighttime data (where GEP is zero and $NEE = ER$). The soil temperature was measured at 5 cm in depth since the best relationship r^2 value was recorded here.

For longer daytime gaps in growing seasons, a hyperbolic relationship between NEE and PPFD was used:

$$NEE = \frac{\alpha * PPFD * P_{max}}{P_{max} + \alpha * PPFD} - ER \quad (4)$$

where α is the initial slope of the curve, P_{max} is the maximum gross productivity, and $PPFD$ is the photosynthetic photon flux density.

3.3.2 Reservoir data

There are many factors that can affect CO₂ flux of a waterbody. Thus, instead of using a regression technique, a semi-empirical method was used to fill the gaps in reservoir data to make sure that the gap-filling strategies fit local environmental conditions well.

During gap-filling (Figure 3.2), three condition variables were listed (Lasslop et al., 2010):

1. Only the data of direct interest are missing;
2. Given condition 1, air temperature or vapour pressure deficit is missing, too;
3. Given condition 2, radiation data is missing, too;

In case 1, the missing data is simply replaced by the mean value under similar meteorological conditions within a time interval of \pm seven days. If there is no satisfying similar meteorological condition, expand the time interval to \pm 14 days. In case 2, approach the same way as case 1. However, a similar meteorological condition can be defined only when global radiation deviation is less than 50 W m⁻². In case 3, the missing data is interpolated, starting from \pm 0.5 h. If all these three cases could not fill the data, the procedure is repeated with an increased window size until the gap can be filled.

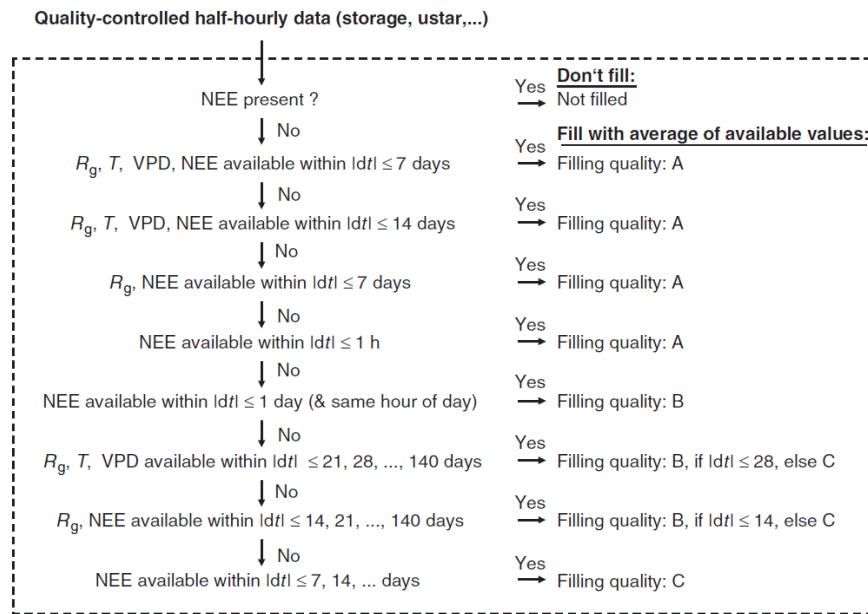


Figure 3.2 Empirical approach gap-filling algorithm (Lasslop et al., 2010)

4. RESULTS

4.1 Meteorological facts of two data sites

4.1.1 Temperature at forest site

The study site has a typical sub-arctic continental climate characterized as fully humid, snow-dominated long winters and cool short summers. The annual mean air temperature in the six-year study period was 1.3 °C with occasionally extreme cold daily temperature below -30 °C; the minimum daily temperature (-35.5 °C), took place on day count 659, or Jan 14th, 2009. Air temperature tended to be more extreme than soil temperature. The annual mean soil temperature was 4.2 °C; the minimum daily temperature (-5.4 °C) took place on day count 677, or Feb 1st, 2009. In general, the annual minimum temperature took place in January, and the annual maximum temperature took place in July or August. For the warmest two to three months, air temperature fluctuated between 10 °C and 23 °C, the soil temperature was a bit cooler, fluctuated in the range of 10 °C to 15 °C.

	08 _{air}	08 _{soil}	09 _{air}	09 _{soil}	10 _{air}	10 _{soil}	11 _{air}	12 _{soil}
Jan.	-15.4	-0.2	-24.4	-4.4	-14.7	-2.3	-18.6	-0.4
Feb.	-19.4	-0.3	-16.9	-3.1	-9.3	-1.8	-18.2	-1.6
Mar.	-14.9	-0.6	-12.1	-1.4	-6.5	-1.3	-11.8	-1.4
Apr.	-0.3	0.0	-1.6	0.0	2.9	0.0	-2.0	-0.2
May	5.5	1.8	3.2	0.1	9.5	1.6	7.0	0.4
Jun.	14.0	10.6	15.3	8.6	12.0	7.6	15.0	8.8
Jul.	15.8	13.0	16.4	12.1	17.2	12.4	16.5	11.9
Aug.	16.5	13.9	13.7	11.5	15.8	12.7	15.5	12.6
Sept.	10.5	10.4	11.0	9.8	9.7	9.6	10.6	9.9
Oct.	3.8	5.5	2.2	4.5	2.7	5.2	5.7	6.7
Nov.	-2.6	0.2	0.1	2.4	-2.6	1.9	-2.6	2.5
Dec.	-17.9	-3.	-13.6	-1.2	-8.6	0.4	-14.8	-0.6

It can be observed (Figure 4.1) that the trend of soil temperature is "fitting along" the pattern of air temperature when the temperature is above 0 °C. When the temperature is

below 0, the soil temperature is more constant compare to air temperature due to better heat insulation and preservation by snow cover. During the early spring of every study year, soil temperature remained steady at 0 °C for a couple of weeks due to ice-melting, an isothermal phase-changing process. After the melting of snow, soil temperature increased dramatically by 4 °C - 8 °C.

There is a time lag of temperature increase and decrease between air and soil (Figure 4.1), where the soil was heated up or cooled down later than air due to higher water content and thus higher heat capacity. This time lag in temperature is best observed when both the temperature of soil and air are above 0 °C.

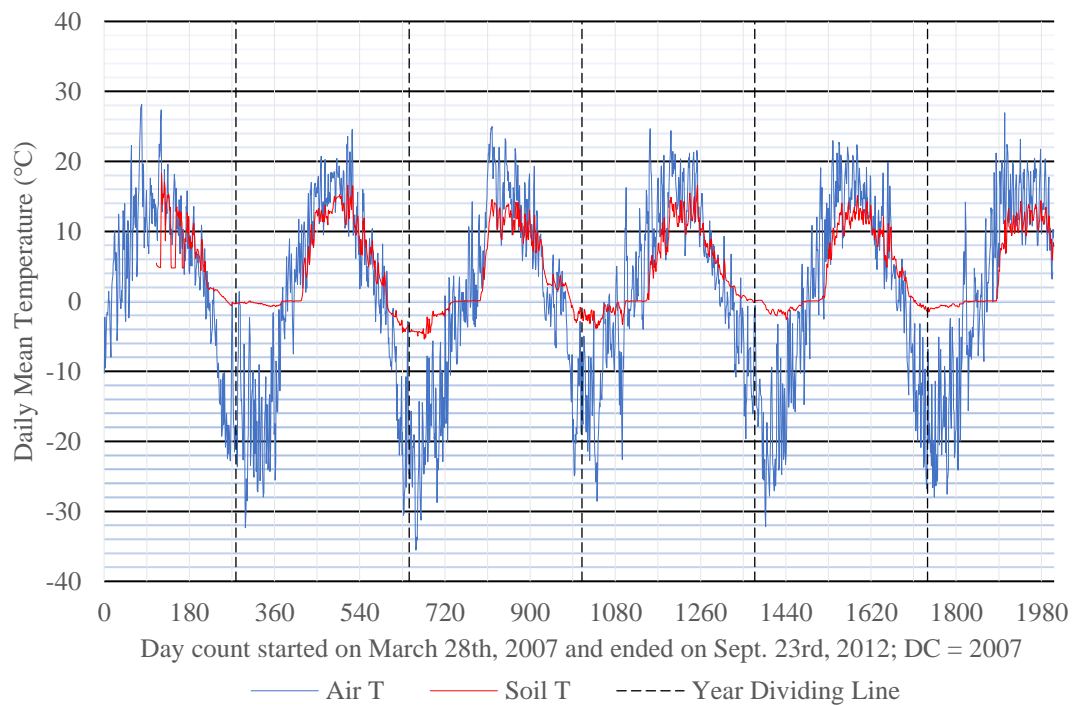


Figure 4.1 Daily averaged air and soil temperature at the forest site; T_a (°C) air temperature, T_s (°C) soil (ground) temperature from March 28th, 2007 to September 23rd, 2012

4.1.2 Temperature at reservoir site

The reservoir has a similar climate as the forest. With long, harsh winters and short cool summers, the reservoir experiences significant temperature shifts annually. Different

from the forest site, the air temperature change at the reservoir site is a bit more moderate with less cold minimum daily temperature but cooler maximum daily temperature (Table 4.2). This is as expected because of a combination of water moderating the extremes local climate and stronger winds in the exposed reservoir area cooling the environment. The annually mean temperatures of the four gap-filled years (2008, 2009, 2011, 2012) are -0.73 °C, -2.26 °C, -1.07 °C and -0.19 °C, respectively. The daily mean air temperature is fluctuating between -26 °C and 19 °C throughout each year (Figure 4.2), with instant 30-min air temperature extrema of below -30 °C or above 22 °C occasionally.

Year	Minimum	Maximum	Mean
2008	-31.5	22.1	-0.7
2009	-31.3	22.1	-2.3
2011	-31.4	22.2	-1.1
2012	-30.9	22.1	-0.2

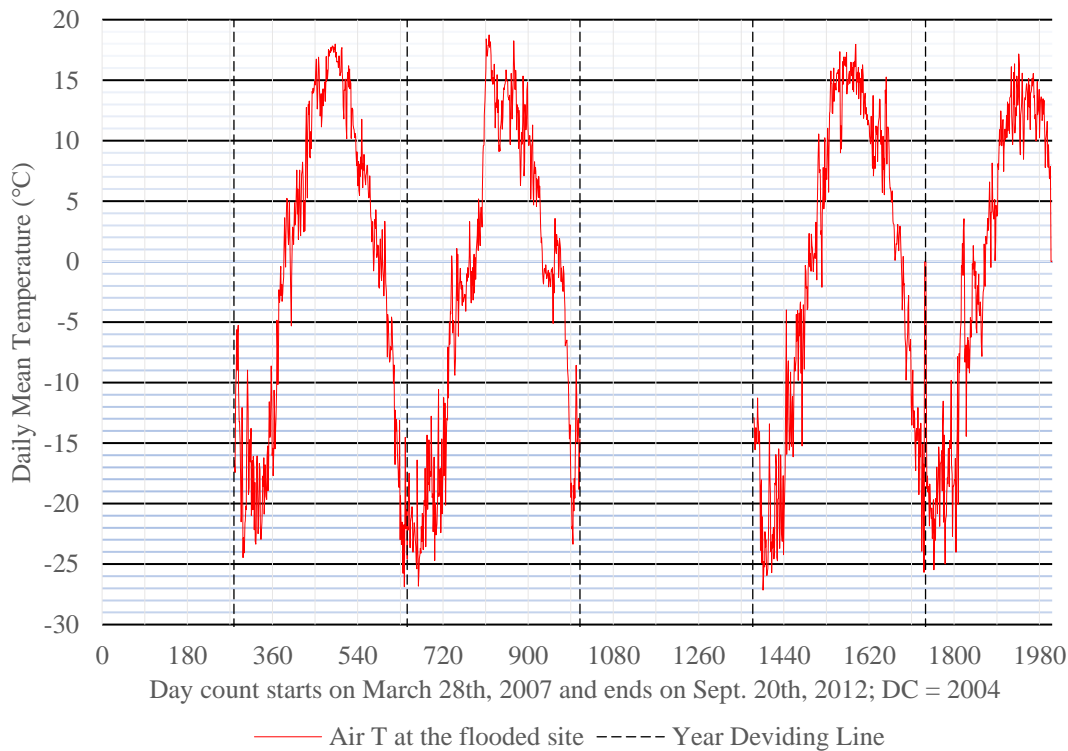


Figure 4.2 Daily averaged air temperature (°C) of the reservoir site for 2008, 2009, 2011

and 2012

4.1.3 Wind characteristics

The gap-filled wind direction and speed data at the reservoir site were used for wind property of two study sites because more homogeneous conditions above the reservoir can reveal more appropriate wind behaviour imagery of the whole Eastmain-1 area. Overall gap-filling performance of six-year wind speed and direction shows 87% of gap-filled useful data. If excluding 2007's data, the percentage of useful data reaches 94%.

Year	R	NaN	% useful	Year	R	NaN	% useful
2007	6132	7153	46 %	2010	16731	789	96%
2008	15351	2271	87 %	2011	16806	714	96%
2009	16373	1147	93 %	2012	12434	301	98%

Note: “R” implies useful real number; “NaN” implies data empty, or gap; % of useful data calculated by $R/(R+NaN)$

The characteristics of wind at the study site were demonstrated by six wind rose figures (Figure 4.3). Winds were least common from the northeast and generally, the prevailing wind was southerly. The majority of sector bars occupied 115° to 345° (SE to SW).

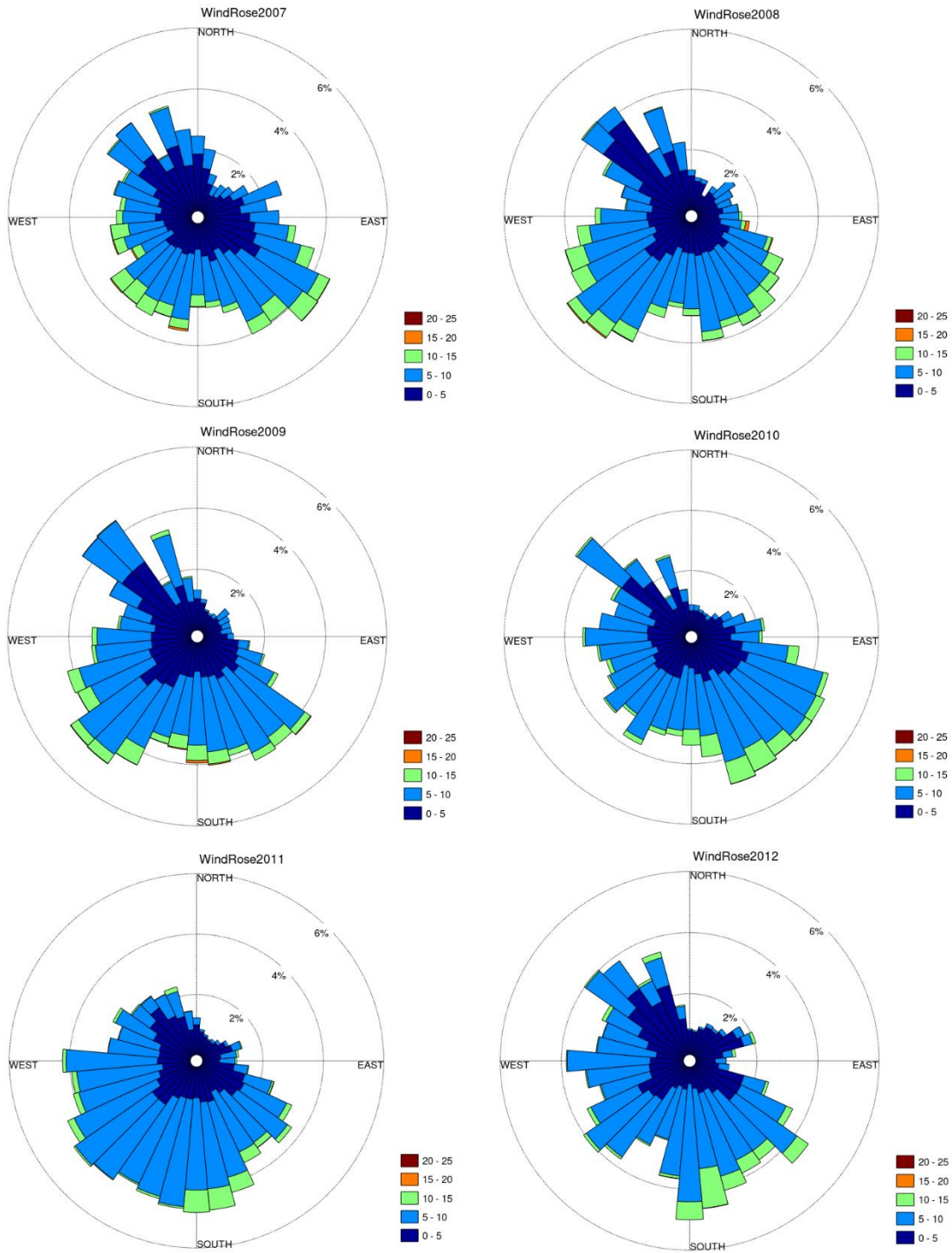


Figure 4.3 Wind rose of Eastmain-1 reservoir wind direction and intensity (speed), annually

4.2 Net Ecosystem Exchange pattern of forest site

The net ecosystem exchange (NEE) in forest site is calculated as the difference between ecosystem respiration (ER) and gross ecosystem production (GEP). A positive value of NEE implies a net release of CO₂ from the ecosystem to the atmosphere, and vice versa.

4.2.1 Diurnal and Monthly pattern of NEE

Throughout six study years, a typical characteristic of forest NEE is that it has a clear diurnal pattern of daytime CO₂ uptake and nighttime CO₂ release (Figure 4.4a-f). Due to peak temperature and solar radiation, July and August are the two months with the highest diurnal differentiation between daytime and nighttime throughout the six study years. The peak CO₂ uptake flux density, or most negative NEE, are in these two months; the peak values take place between 10 am and 14 pm are often between -6 $\mu\text{mol m}^{-2}\text{s}^{-1}$ and -9 $\mu\text{mol m}^{-2}\text{s}^{-1}$. The nighttime NEE is also maximized during each year's July and August, and ranges from 2 $\mu\text{mol m}^{-2}\text{s}^{-1}$ to 4 $\mu\text{mol m}^{-2}\text{s}^{-1}$ due to warm temperature for nighttime respiration. Note that July and August are often the two months with the highest mean air and soil temperature (Table 4.1). Moving apart from July and August, the flux density of daytime and nighttime NEE gradually decreases in absolute quantity, implies a weakening of both daytime CO₂ uptake (photosynthesis) and nighttime release (respiration).

Year	Jan.	Feb.	Mar.	Apr.	May.	Jun.	Jul.	Aug.	Sept.	Oct.	Nov.	Dec.
2007	n/a	n/a	n/a	-0.05	-0.88	-1.27	-1.50	-0.78	-0.46	-0.01	0.25	0.10
2008	0.76	0.78	0.74	0.30	-0.97	-0.89	-1.17	-0.83	-0.71	0.11	0.64	0.61
2009	0.41	0.46	0.46	0.18	-0.41	-1.06	-1.44	-1.47	-0.46	-0.02	0.59	0.56
2010	0.33	0.31	0.31	-0.13	-0.93	-1.52	-0.87	-0.46	-0.28	0.05	0.57	0.52
2011	0.45	0.37	0.36	0.17	-0.65	-1.35	-1.80	-1.32	-0.28	-0.09	0.51	0.43
2012	0.28	0.30	0.29	0.05	-0.92	-1.14	-1.21	-0.96	-0.24	n/a	n/a	n/a

Note: Gray blocks imply a net monthly release while light green blocks imply a net monthly uptake of CO₂

Numerically, it can be observed (Table 4.4) that the ecosystem has a net monthly CO₂ uptake (negative NEE) between May and September; April and October are transition months and could have net uptake during warmer years. It is worthy to note that 2008 seemed to have a warmer winter implied by higher NEE flux density from January to March. The warm winter can also be observed from the temperature data (Table 4.1) where the monthly mean temperature of the soil at the forest site during January to April is constantly above -1 °C. The growing season is approximated (Table 4.5) when daily mean temperature constantly (for at least five consecutive days) reaches 4 °C and 0 °C for air and soil surface, respectively (Lemieux, 2010). There is a strong relationship between growing season and net CO₂ uptake due to warm temperature, ample solar radiation and forest growth.

Year	Starting DOY and date	Ending DOY and date	Growth season length
2007	102; April 12th	304; October 31st	202
2008	106; April 15th	302; October 28th	196
2009	125; May 5th	285; October 19th	160
2010	90; March 31st	301; October 28th	211
2011	111; April 21th	319; November 15th	208
2012	121; April 30th	302; October 28th	181

Note: the ending date and length of 2012 (darkened units) are estimated by averaging the previous five years' data

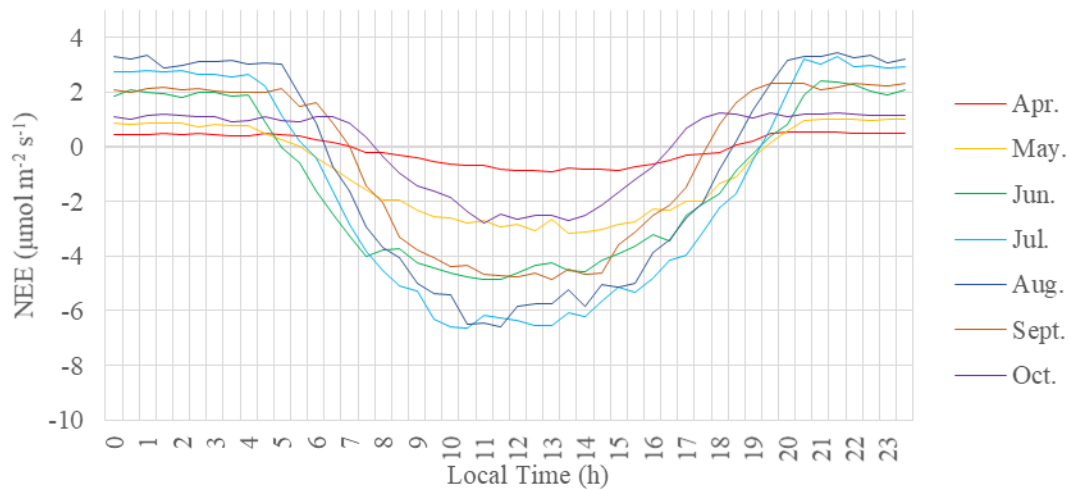


Figure 4.4a Diurnal NEE ($\mu\text{mol m}^{-2} \text{s}^{-1}$) variation at the forest site in 2007

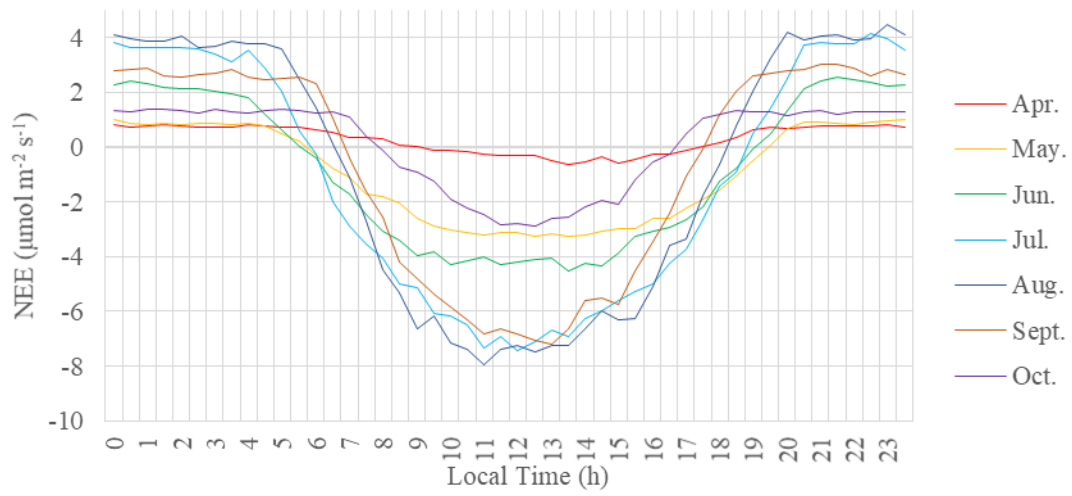


Figure 4.4b Diurnal NEE ($\mu\text{mol m}^{-2} \text{s}^{-1}$) variation at the forest site in 2008

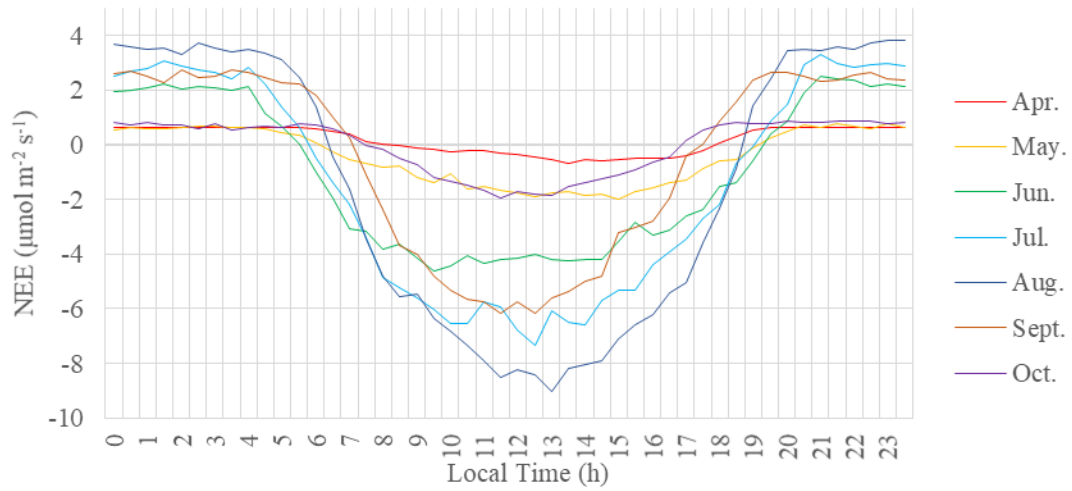


Figure 4.4c Diurnal NEE ($\mu\text{mol m}^{-2} \text{s}^{-1}$) variation at the forest site in 2009

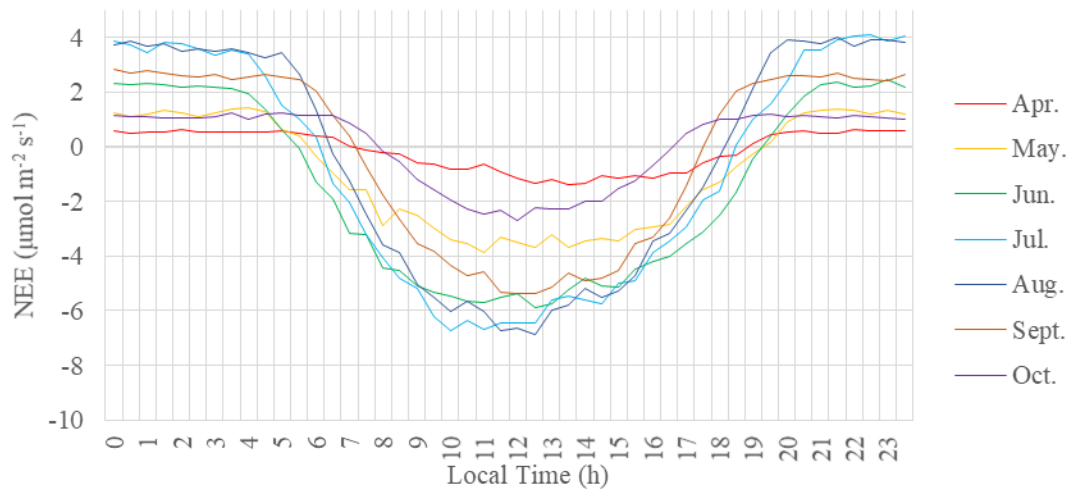


Figure 4.4d Diurnal NEE ($\mu\text{mol m}^{-2} \text{s}^{-1}$) variation at the forest site in 2010

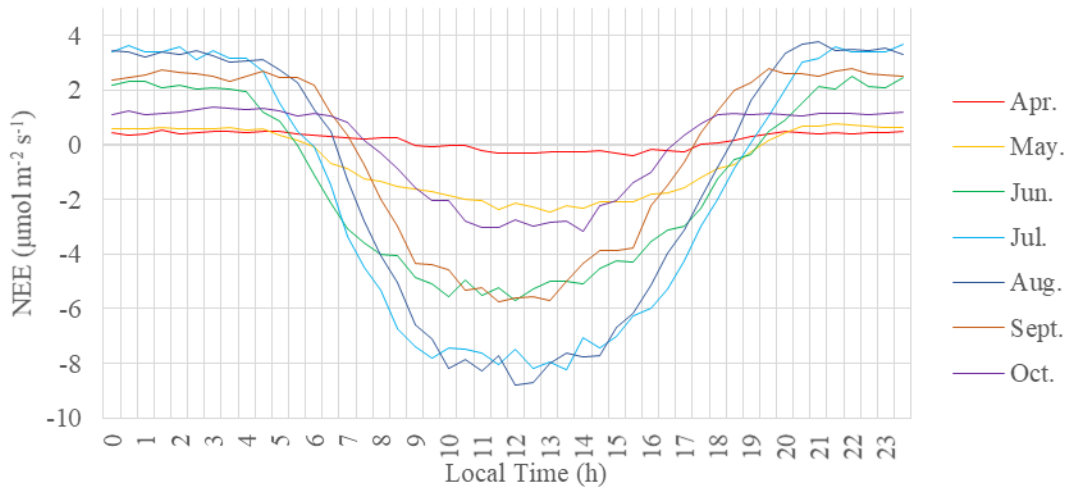


Figure 4.4e Diurnal NEE ($\mu\text{mol m}^{-2} \text{s}^{-1}$) variation at the forest site in 2011

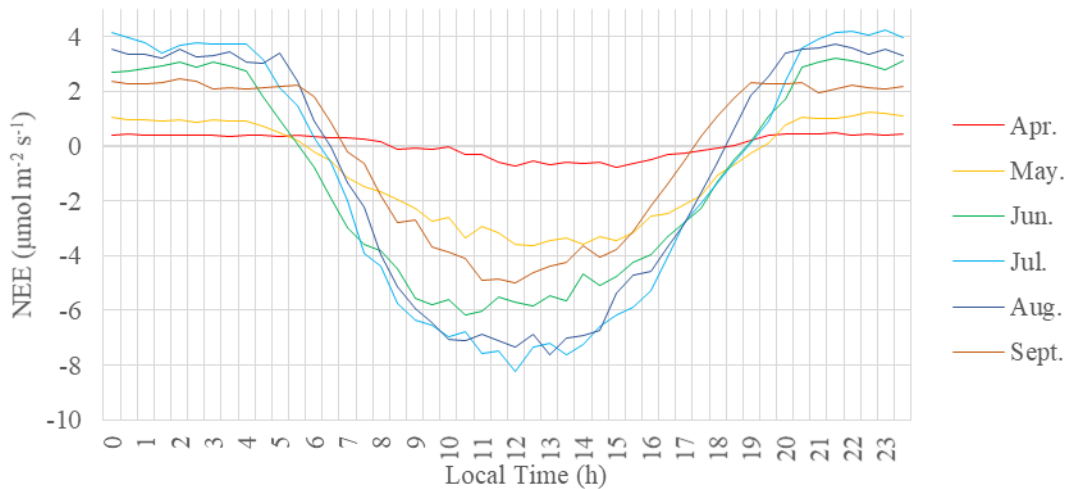


Figure 4.4f Diurnal NEE ($\mu\text{mol m}^{-2} \text{s}^{-1}$) variation at the forest site in 2012

4.2.2 Annual pattern of NEE

NEE follows a seasonal pattern consistently throughout six study years (Figure 4.5). The NEE is bell-shaped during each year's growing season, with the most negative value in the middle of July and August, when the highest intensity of photosynthesis takes place. During non-growing seasons, specifically, early November to end of March, the NEE is constantly positive with a slightly descending trend from $1 \text{ g C m}^{-2} \text{d}^{-1}$ to $0.5 \text{ g C m}^{-2} \text{d}^{-1}$ due to gradual decline in ecosystem respiration activities. For example, during late winter and

early spring of 2008, the NEE maintained a constant emission of about $1 \text{ g C m}^{-2}\text{d}^{-1}$. Meanwhile, the soil temperature of this period is constantly around $0 \text{ }^{\circ}\text{C}$, with very little fluctuation. It is highly likely that the precipitation, primarily snow, was ample enough for the soil to maintain a relatively warm temperature and made it possible for constant ecosystem respiration level.

There are occasionally positive NEE values during growing seasons, and most of them exceeded $1 \text{ g C m}^{-2}\text{d}^{-1}$. This unusual phenomenon could be caused by days with reduced sunlight (PPFD) such as days with precipitation (Figure 4.6). On such days, respiration can exceed photosynthesis. These events were particularly frequent in 2010 and 2012, where low PPFD and positive NEE can be spotted. However, as further analysis of cumulative NEE discussed, these temporal events have a very limited impact on the whole picture of annual NEE.

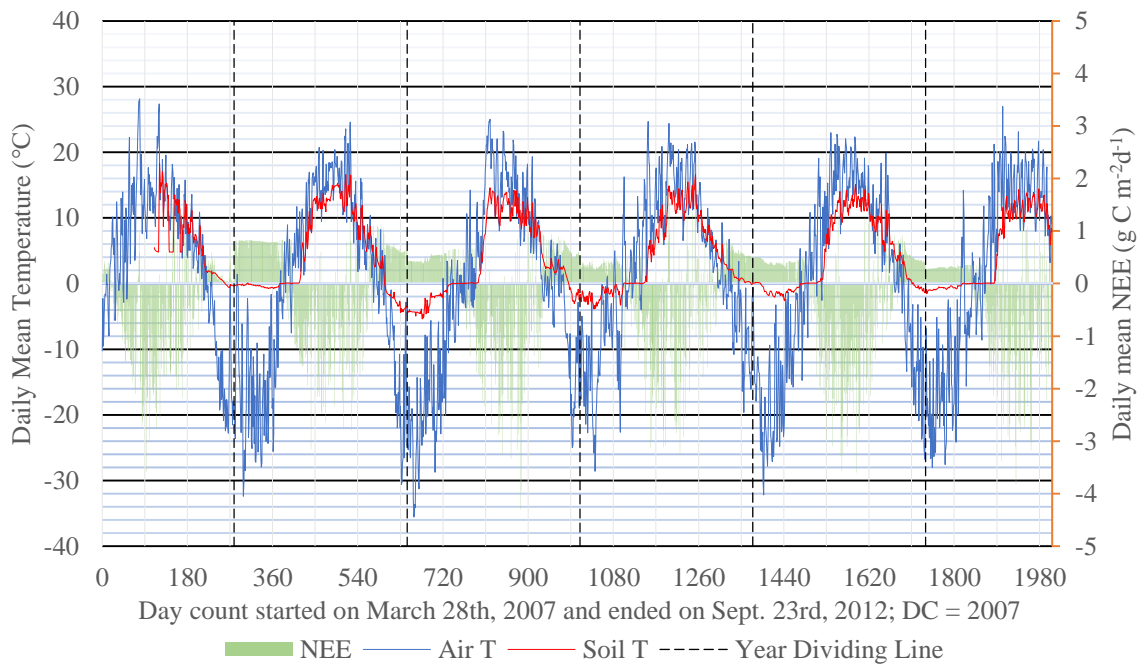


Figure 4.5 Relationship between air and soil surface temperature ($^{\circ}\text{C}$) and NEE ($\text{g C m}^{-2}\text{d}^{-1}$) at the forest site

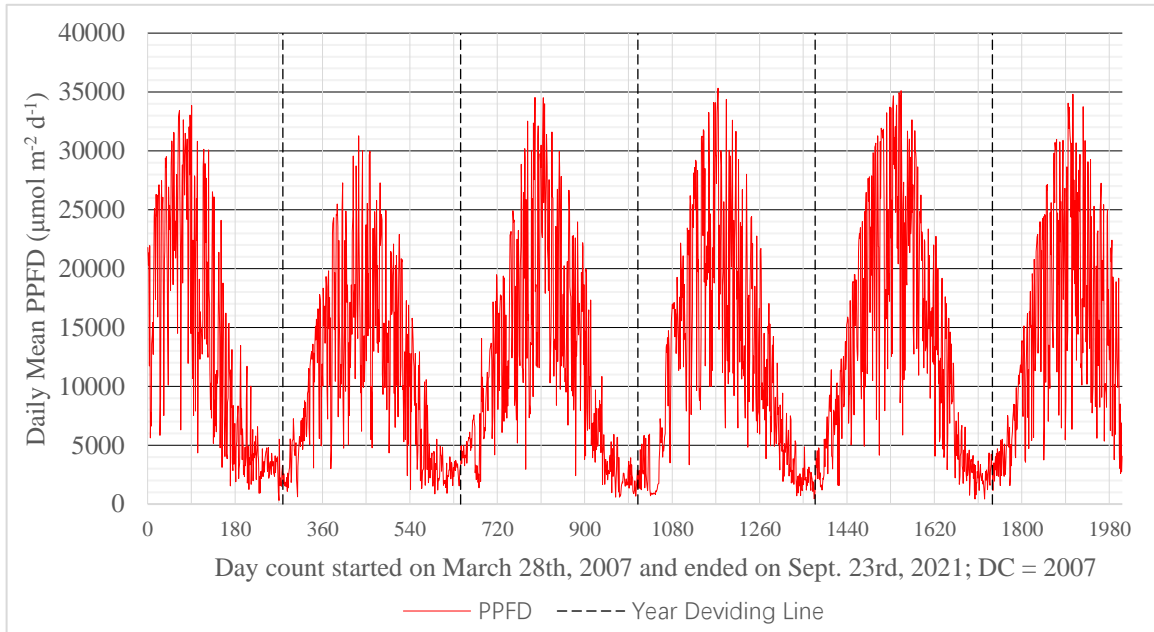


Figure 4.6 Daily (sum of the 30-minute averaged PPFD at the forest site for six study years

4.2.3 Cumulative pattern of NEE

The cumulative pattern of each year's GEP and ER can be approximately described as logistic curve. There are two points on each of the cumulative ER and GEP curves where the slope changes significantly, coinciding with the beginning and the end of the growing season. ER initially has a constant positive slope and gradually increase due to weak but constant soil respiration during winter. The slope then becomes higher when entering the growing season mainly due to enhanced soil and plant respiration, steepening the curve. The slope then returns to a small positive magnitude similar to the first stage after exiting the growing season.

Cumulative GEP is always increasing faster than ER and at the end of each year, GEP magnitude is always greater than ER (Figure 4.7), leading to an annual negative cumulative NEE that implies a net uptake of CO₂ at the forest site. The slope of GEP prior to and after the growing season is approximately zero because there is no photosynthesis during winter. The annual NEE at forest site for 2008 to 2011 is -21, -71, -68 and -103 g C m⁻² yr⁻¹ respectively. Because the data of 2012 from DOY 266 to 366 is not available, the annual

cumulative flux of 2012 is estimated by taking the average value of the previous five years' data from DOY of 266 to 365. Then add a "shifting adjustment parameter" calculated by the sum of flux difference between DOY 265 and 266 (ER 29.93 g C m⁻² d⁻¹, GEP 37.53 g C m⁻² d⁻¹), and the five-day-averaged daily flux change between DOY 261 and DOY 265 (ER 3.63 g C m⁻² d⁻¹, GEP 2.17 g C m⁻² d⁻¹).

Year	2008	2009	2010	2011	2012(est.)
GEP	617	556	606	593	631
ER	596	485	539	490	545
NEE	-21	-71	-68	-103	-86

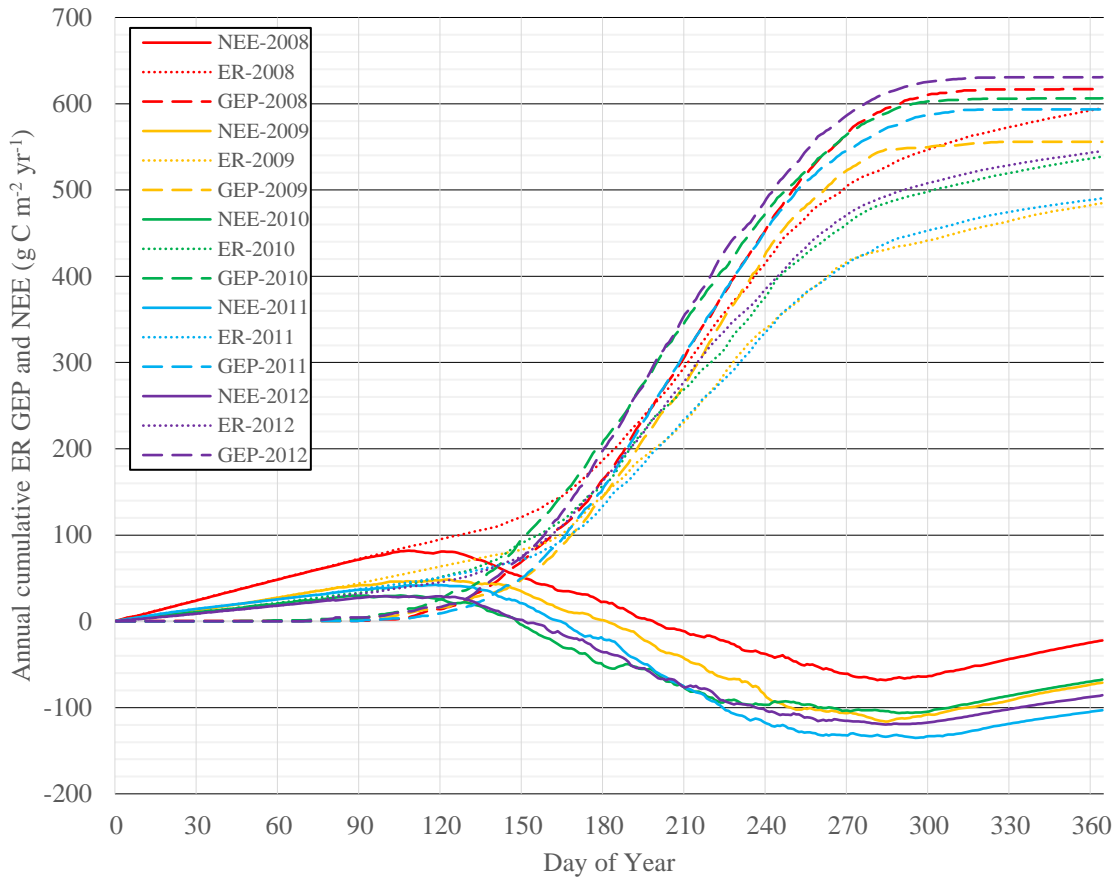


Figure 4.7 Annual cumulative ER, GEP and NEE at the forest site for 2008-2012

4.3 CO₂ pattern of flooded site

4.3.1 Diurnal and monthly CO₂ flux pattern of flooded site

There is no observable diurnal CO₂ flux pattern at the flooded site (Figure 4.8a-d). For most of the time, the monthly averaged 30-min CO₂ flux throughout a day is approximately a horizontal line, indicates that the daily CO₂ flux is relatively constant. Note that the flooded site has a moderate daily temperature because of the high heat capacity of liquid water and evaporation. In addition, there is no or very little photosynthesis going on, so the PPFD parameter becomes less important to the NEE. However, there are some exceptions. For example, July and October of 2009 seem to have a valley-shaped diurnal pattern with low CO₂ flux during daytime and relatively high CO₂ flux during nighttime, ranges from 0.3 $\mu\text{mol m}^{-2}\text{s}^{-1}$ to 1 $\mu\text{mol m}^{-2}\text{s}^{-1}$, and 0.7 $\mu\text{mol m}^{-2}\text{s}^{-1}$ to 1.3 $\mu\text{mol m}^{-2}\text{s}^{-1}$, respectively. Still, these flux differences are not comparable to the diurnal pattern at the forest site, while the pattern of later has a much larger variation range from -9 $\mu\text{mol m}^{-2}\text{s}^{-1}$ to 4 $\mu\text{mol m}^{-2}\text{s}^{-1}$.

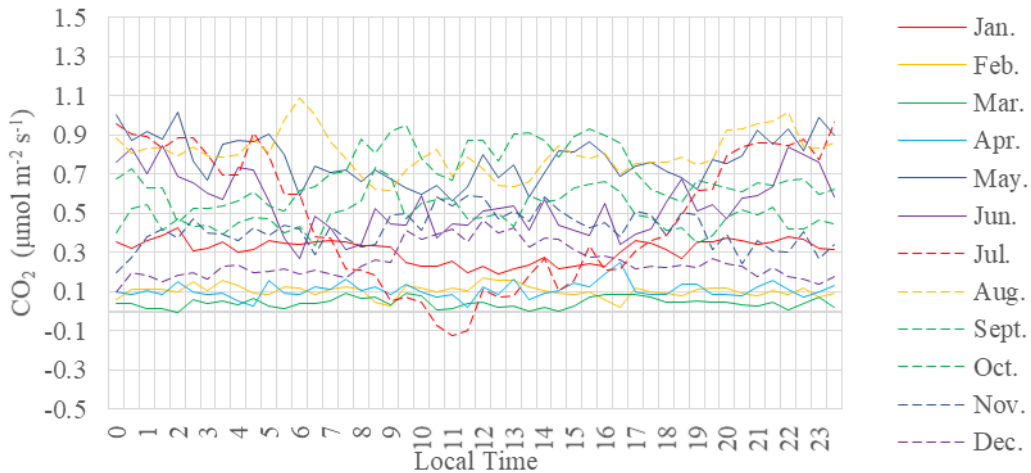


Figure 4.8a Diurnal CO₂ flux at the flooded site in 2008

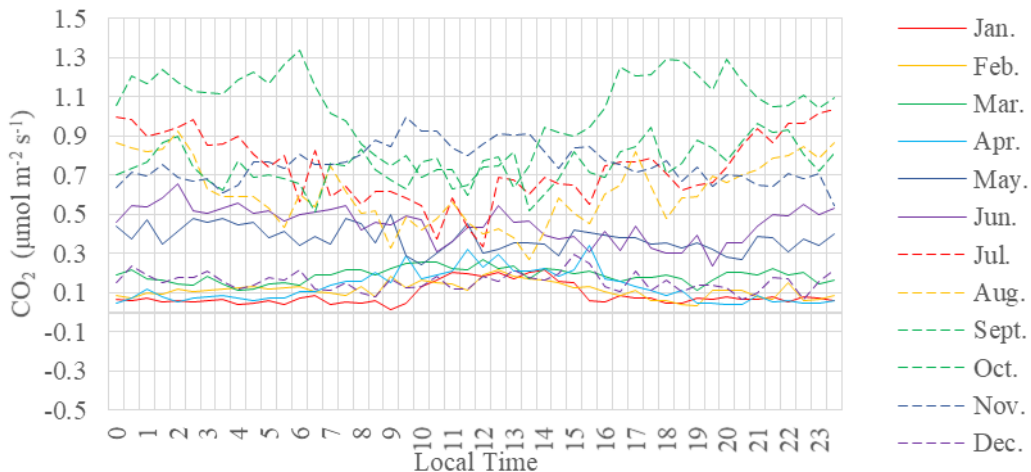


Figure 4.8b Diurnal CO₂ flux at the flooded site in 2009

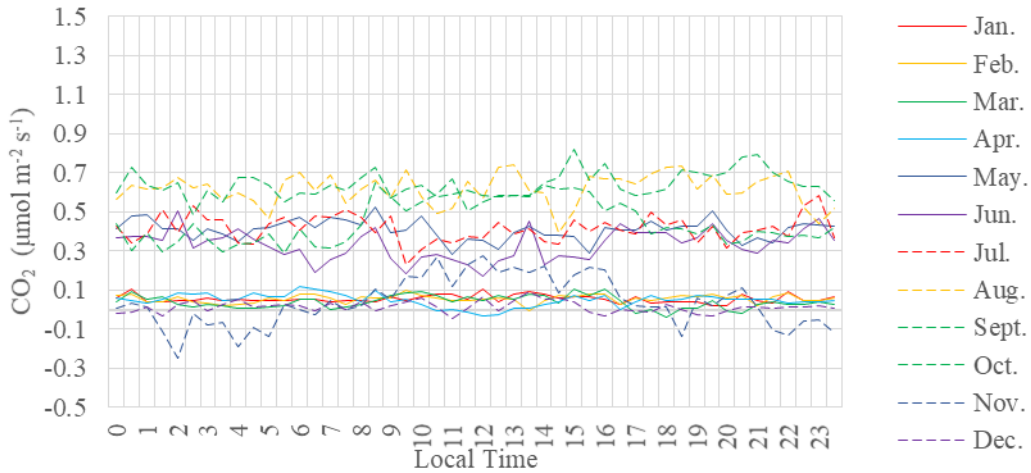


Figure 4.8c Diurnal CO₂ flux at the flooded site in 2011

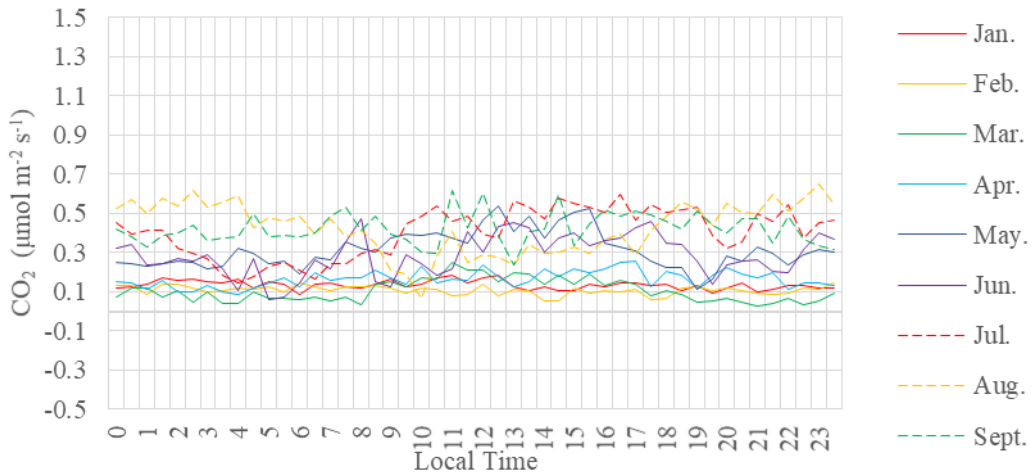


Figure 4.8d Diurnal CO₂ flux at the flooded site in 2012

While there is no diurnal pattern of flooded site CO₂ flux, the monthly difference can be observed clearly. Throughout four gap-filled datasets, the CO₂ flux minima take place in each year's January, February, March, April and December, whereas the maxima take place in August, September and October.

There are several flux peaks throughout each year that a consistent trend can be observed. In each year's May (DOY 140 ± 10), the first and usually largest CO₂ flux release from the flooded area takes place. In 2008, 2009 and 2011, this peak goes beyond $1.5 \mu\text{mol m}^{-2} \text{s}^{-1}$ where in 2012 the peak value is around $1.3 \mu\text{mol m}^{-2} \text{s}^{-1}$. This is the most consistent

trend throughout 4 study years that can be observed (Figure 4.9, Figure 4.10). The peak starts to form on DOY 130 and restores to normal level on DOY 150, remains high, but fluctuates for 20 days. Prior to this dramatic flux increase, the CO₂ flux during the winter period is consistently small, varies within 0 μmol m⁻²s⁻¹ and 0.5 μmol m⁻²s⁻¹. When the winter period ends, ice starts to melt. CO₂ that has been trapped and stored in the water suddenly releases out into the atmosphere once the ice breaks. Air temperature increase could lead to the rise of water temperature by conduction and encourage more CO₂ stored in water to be released because of CO₂ saturation.

The second flux peak is observed during late August and Early September (DOY 250 ± 20). This peak corresponds closely to autumn reservoir turnover, when air temperature starts the cool and cools the surface water as well, subsequently increase the convective water fluxes and force the vertical water exchange. Mixing of the water column at the flooded site encourages more release of CO₂ that is originally stored in deep water. However, this peak has a lower magnitude than the first peak during ice break in May.

There are some inconsistencies between different years that are worthy to note. For 2008 and 2009, there seems to be an additional peak during late October and early November (DOY 300 ± 10). For 2009, a constant plateau-shaped peak takes place during late July (DOY220), and CO₂ flux remains high at around 1.2 μmol m⁻²s⁻¹ for two weeks. For 2009 and 2011, there is a negative CO₂ flux that indicates an uptake in early December, probably due to CO₂ absorption of cold water and locked by water freeze.

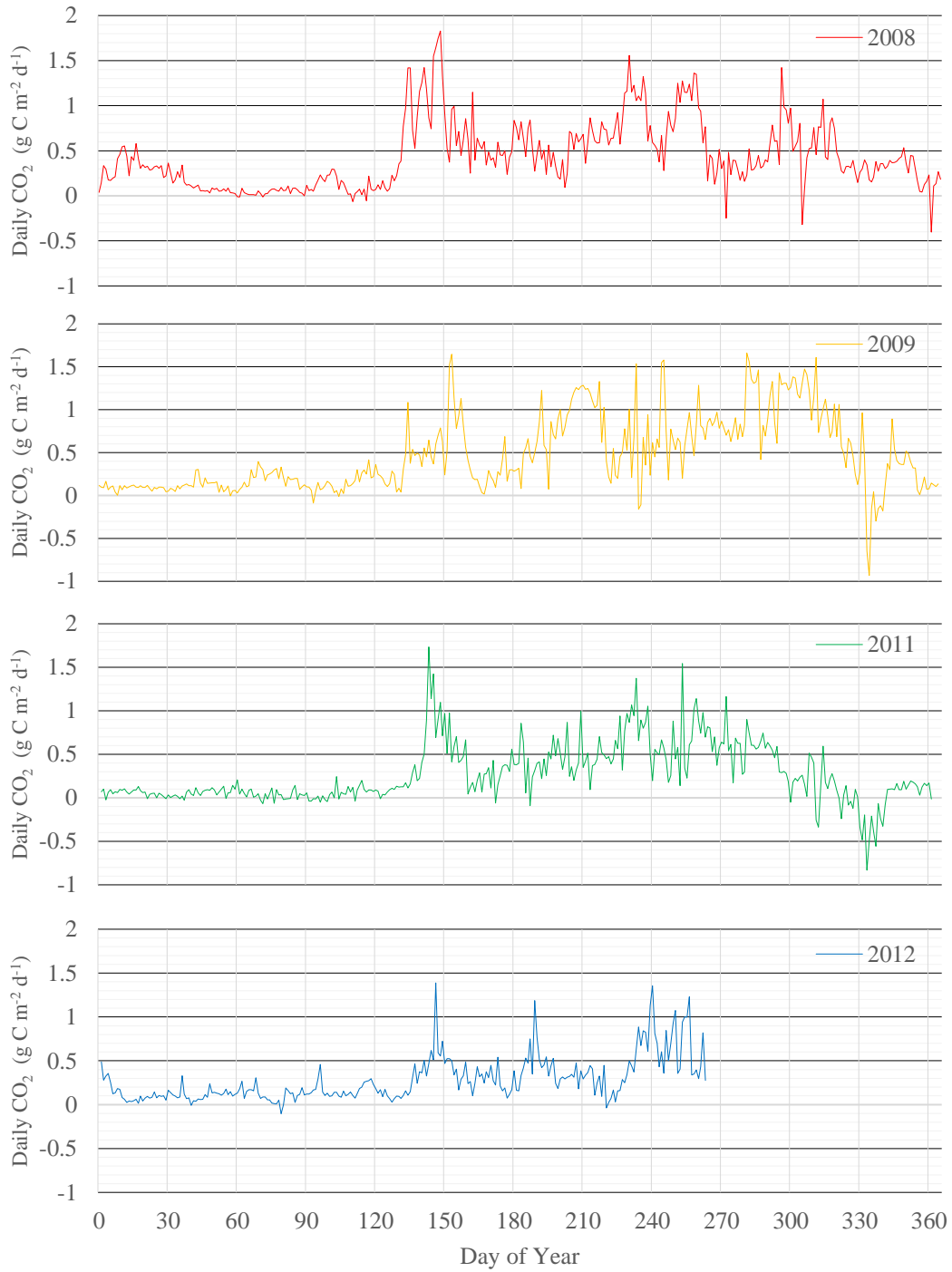


Figure 4.9 Daily averaged CO₂ flux for 2008 2009 2011 and 2012

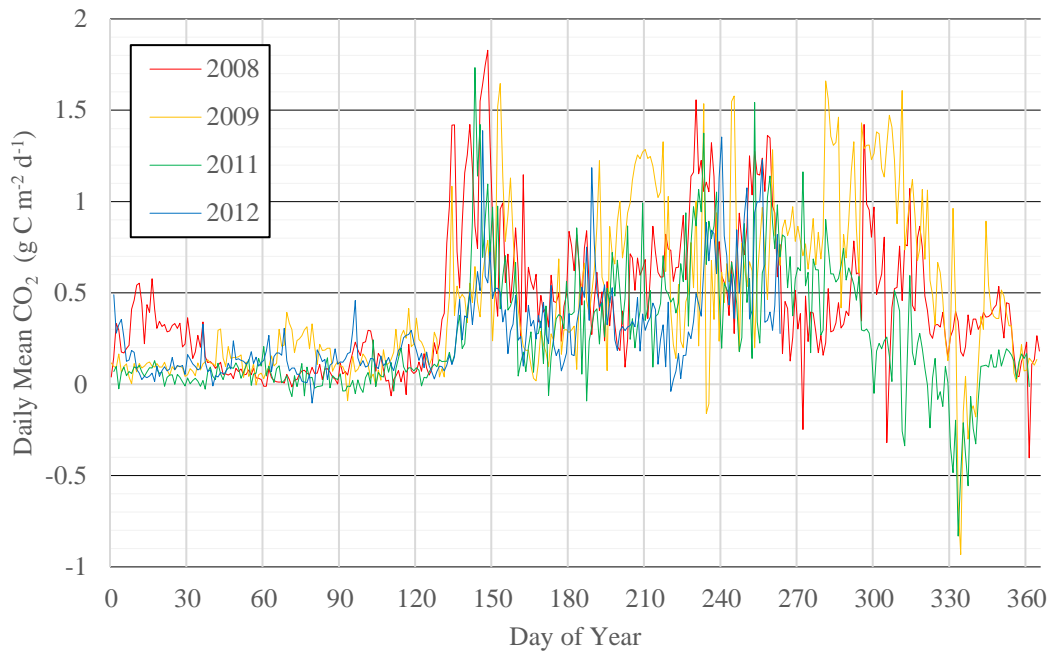


Figure 4.10 Daily averaged CO₂ flux at the flooded site for 2008 2009 2011 and 2012 (combined)

4.3.2 Annual cumulative CO₂ flux pattern

Like the forest site, the daily averaged CO₂ flux of 2012 after September 20th is estimated by taking the average value of the previous three years' data from DOY of 266 to 365 and adding a "shifting adjustment parameter" (-25.881) to connect the estimated curve to DOY 265 of 2012.

The annual cumulative CO₂ flux pattern of the flooded site is pretty consistent. Cumulative CO₂ flux (Figure 4.11) shows the four increasing non-negative curves of 2008, 2009, 2011 and 2012, in which the result of annual CO₂ emission (Table 4.7) ranges from 98 g C m⁻²yr⁻¹ to 171 g C m⁻²yr⁻¹. The data indicates that the flooded site is a net source of CO₂ to the atmosphere.

Year	2008	2009	2011	2012(265)	2012(est.)
CO ₂	160	171	98	74	117

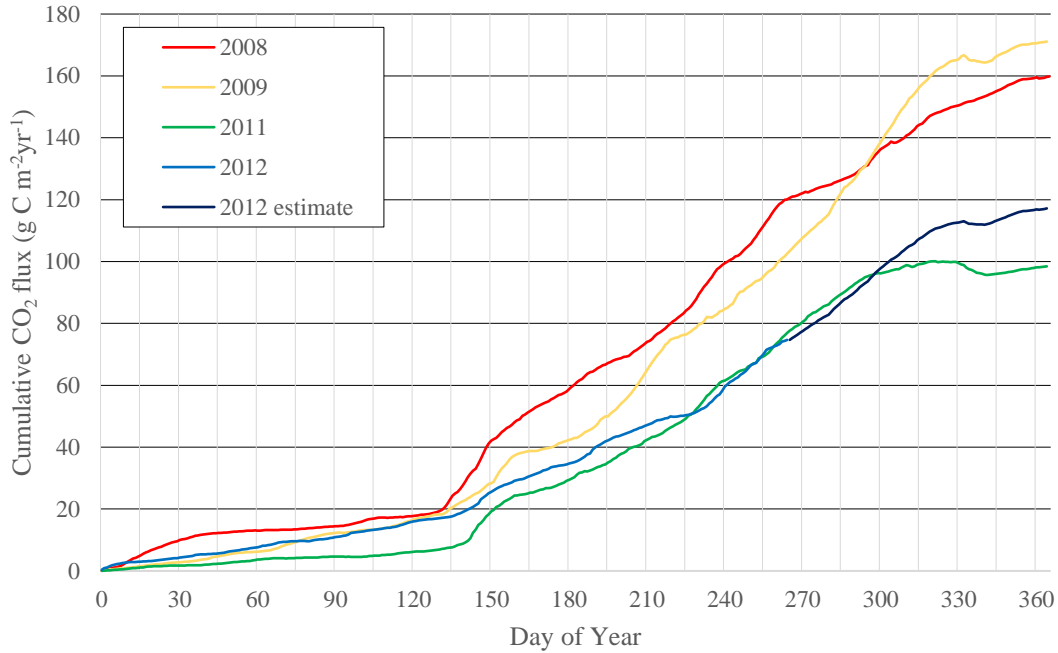


Figure 4.11 Cumulative CO₂ flux at the flooded site. The portion of 2012 indicated by the green line is the estimated flux found by averaging the previous three years

4.4 Net effect of the reservoir

The net reservoir effect for each study year is calculated by:

$$Net\ Effect = CO_{2reservoir} - NEE_{forest} \quad (5)$$

The absence of data after September 2012 is filled by estimation, as mentioned before. For the four years, the net NEE is always positive and ranges from 181 g C m⁻²yr⁻¹ to 242 g C m⁻²yr⁻¹ (Table 4.8). Annually, therefore flooding a forest that is taking up carbon leads to a net increase of CO₂ emission to the atmosphere that is greater than the measured emissions from the reservoir.

If we take a close look to the monthly pattern, the flooded site actually releases less CO₂ during the forest site's non-growing seasons (Figure 4.12); because of weaker ecosystem respiration and the blocking of ice, the net effect is decrease during these periods.

However, this decrease of CO₂ emission is offset by the dramatic increase of reservoir CO₂ emission during the forest site's growing season. During growing seasons, the forest is a carbon sink, whereas the flooded site is a carbon source. Comprehensively, the flooded

site not only offsets the carbon uptake of forest but also adds even more CO₂ to the atmosphere. For a young hydroelectric reservoir like Eastmain-1, this addition of CO₂ ranges from approximately 181 to 242 g C m⁻²yr⁻¹.

Table 4.8 Net effect of reservoir (g C m ⁻² yr ⁻¹)			
Year	NEE_forest	CO ₂ _reservoir	Net Effect
2008	-21	160	181
2009	-71	171	242
2011	-103	98	201
2012(265 days)	-115(+)	74 (-)	189(-)
2012 estimated	-86	117	203

Note: Net effect is calculated by CO₂_reservoir – NEE_forest. |+| and |-| indicates that the value has a greater or smaller absolute value compare to expected annual data

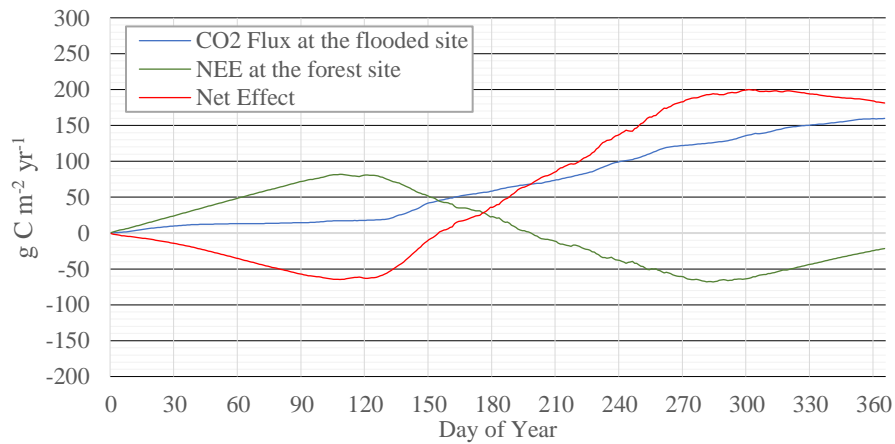


Figure 4.12a Net effect of carbon emission in 2008

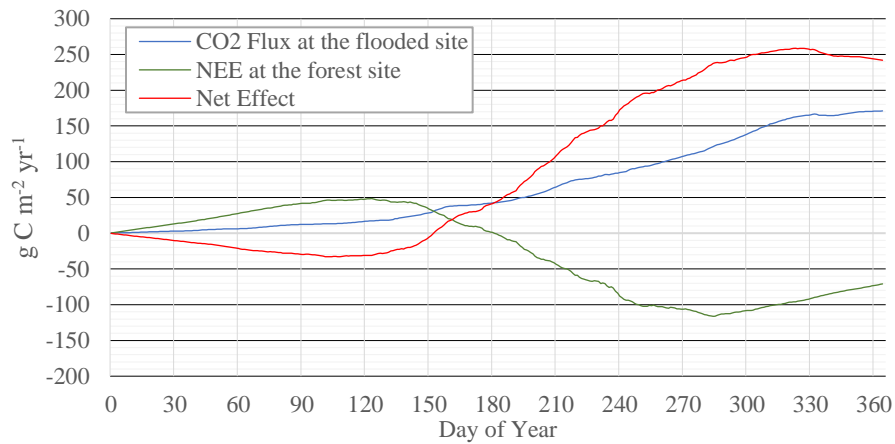


Figure 4.12b Net effect of carbon emission in 2009

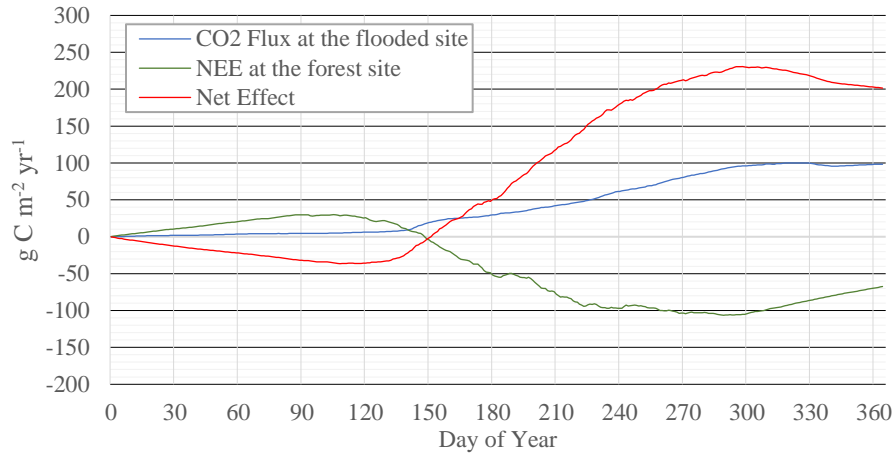


Figure 4.12c Net effect of carbon emission in 2011

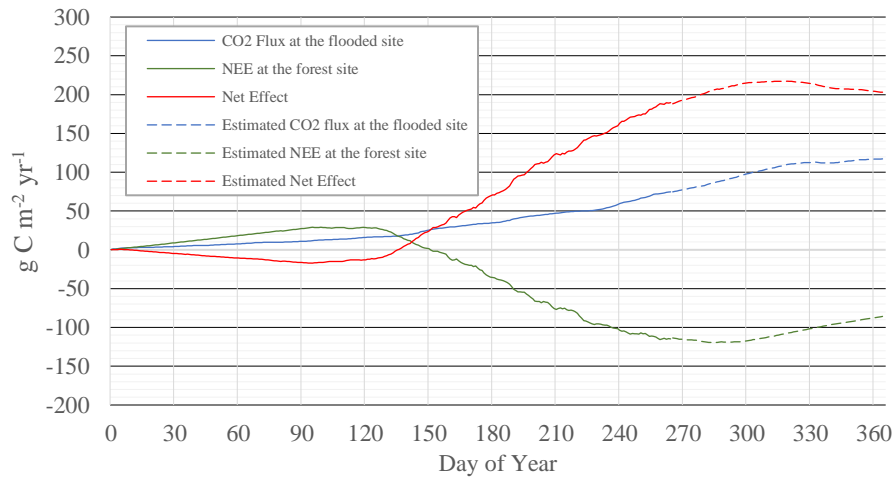


Figure 4.12d Net effect of carbon emission in 2012, the dotted line is the estimated flux for 2012 averaged by the previous three years

5. DISCUSSION

5.1 Flux comparison

5.1.1 Forest NEE

Throughout the six-year study period, the forest acts as a carbon sink, while the reservoir is constantly a carbon source to the atmosphere. The study site Eastmain-1 is in northern Quebec with long, harsh winter and ample snowfall, with typical biophysical properties of Canadian black spruce boreal forest (Lemieux, 2010). The annual NEE from the study black spruce forest is similar to comparable old black spruce (OBS) forests that were previously studied (Table 5.1). The NEE of 2008 is similar to the eastern OBS in Quebec (Bergeron et al., 2007; Payeur-Poirier et al., 2012); higher NEE in subsequent years is higher than the OBS in Manitoba and Saskatchewan, but slightly smaller than a recently harvested juvenile black spruce regrowth in Quebec. Age can be a critical factor to the NEE of a forest (Goulden et al., 2006); the forest in the study site has an average age of 84 (Lemieux, 2010), and summer GEP is higher than annual ER, making it a moderate carbon sink. The small NEE in 2008 is likely caused by ample snowfall and the relatively warmer soil temperature due to snow insulation. The soil respiration during that warm winter is constantly around $1 \text{ g C m}^{-2}\text{d}^{-1}$ for three to four months, and offsets some of the GEP during the summer (Figure 4.5).

Study Site	Study Period	Annual NEE g C	Note	Reference
EM-1 reservoir, Northern Quebec	2007-2012	-21 to -103		Current study
EOBS (Quebec)	2004	-12 to -16		Bergeron, et al., 2007
NOBS (Manitoba)	2004	-16 to -38		
SOBS (Saskatchewan)	2004	-25 to -35		
EOBS (Quebec)	2008	-2 to -10	Pre-harvest	Payeur-Poirier et al., 2012
HBS00 (Quebec)	2008	84 to 90	Recently-harvest	
HBS75 (Quebec)	2008	-108 to -178	Juvenile	
NOBS (Manitoba)	1994-2008	-4 to -48		Soloway et al., 2017

In general, the result from forest site matches the trend of GEP and ER of other old black spruce forests and indicates an annual moderate carbon sink.

5.1.2 Flooded site CO₂ emission

The carbon dioxide emission from the current study ranges from 98.05 to 171.1 g C m⁻²yr⁻¹. This is within the range provided by other studies focusing on the carbon emission of young hydroelectric reservoirs in the boreal area of Quebec and Ontario (Table 5.2). For example, ELARP (Kelly et al., 1994) and Cabonga (Duchemin et al., 1995) have annual carbon emission ranges from 110 to 368 g C m⁻²yr⁻¹ and 32 to 478 g C m⁻²yr⁻¹, respectively, which are fairly similar to the carbon emission behaviour as Eastmain-1. Exceptionally, Eastmain-Opinica (Kelly et al., 1994; Duchemin et al., 1995) has a higher average emission quantity compared to Eastmain-1. Given that the reservoir age is slightly older than Eastmain-1, the age might be one of the determinants of this emission difference.

Table 5.2 Comparison between the present study and northern hydroelectric reservoir CO₂ emission

Location	Reservoir	Area (km ²)	Age (year)	CO ₂ emission mg m ⁻² d ⁻¹	CO ₂ emission g C m ⁻² yr ⁻¹	Reference
Quebec	Eastmain-1	603	1-6	n/a	98 to 171	Current study
	Laforge-1	1000	1-5	2300 (200-8500)	229 (20-846)	Duchemin et al., 1995; Duchemin, 2000
	Robert-Bourassa	2500	12-19	1500 (160-12000)	149 (16-1195)	Kelly et al. 1994; Duchemin et al. 1995; Duchemin 2000
	Eastmain-Opinica	1000	12-13	3450 (2200-4300)	343 (219-428)	Kelly et al., 1994; Duchemin et al., 1995; Duchemin, 2000
	Cabonga	400	68-70	1400 (320-4800)	139 (32-478)	Duchemin et al., 1995; Duchemin, 2000
Ontario	ELARP	0.2	4	2000 (1100-3700)	199 (110-368)	Kelly et al. 1994

Unfortunately, most of the studies listed followed floating chamber techniques instead of eddy covariance. However, it is still logical to believe that the two methods are comparable in boreal areas (Podgrajsek et al., 2014).

5.2 Study limitations

Ideally, to address the net effect to carbon emission induced from flooding of the boreal forest, the whole process should have proceeded during the study. It includes the measurement of pre-flooded forest NEE and relative biophysical characteristics at the exact flooding area and subsequent measurement of flooded carbon emission behaviour. In reality, however, it is not feasible to execute. Thus, the boreal forest near the flooded site is measured as a substitution. Although the forest site is a typical boreal forest and we assume that the picked forest site is similar biophysically to the pre-flooded forest site, the NEE behaviour of forest site would not be exactly the same as the flooded site prior to the flood due to tiny difference in topography, temporal climate, soil characteristics and biogeography. The error induces from this aspect is indeed inevitable but can be accepted.

On the other hand, the study is locally specific. The emission behaviours of both forest and flooded areas are influenced by climate and biogeography. However, it is still plausible to generalize the result to areas with similar forest characteristics and climate to estimate the net effect that would lead if flooded.

It is also worthy to further investigate the partitioning of ER and GEP of black spruce trees and understories. Reichstein et al. (2005) discussed about the partitioning algorithm from NEE to GEP and ER and emphasized the bias that caused by confounding variables. These variables also exist in current study site and should be addressed if possible.

6. CONCLUSION

There are not many studies addressing the effect on the carbon emission of reservoir impoundment in boreal regions. With increasing of hydropower share in global energy structure, it is of great interest and necessity to research the carbon emission effect of flooding the boreal ecosystem, the largest carbon holder globally.

This thesis describes measurements of the carbon exchange behaviour of the flooded site and an analogical pre-flooded forest site directly using eddy covariance. Six-year continuous flux data from March 2007 to September 2012 were recorded for both sites for subsequent analysis. In all years, the forest site is measured as is a carbon sink while the flooded site is measured as a carbon source.

The NEE of forest site ranges from -21 to -103 g C m⁻²yr⁻¹ throughout four gap-filled years. It is observed that the forest site has a strong seasonal pattern that a net sink is present during growing seasons, and a net source is present during winter. The forest site NEE is highly influenced by solar radiation during growing seasons and has a strong diurnal pattern: uptakes carbon during daytime and releases carbon during nighttime. The seasonal pattern for each year is similar for the forest site across six years.

The CO₂ emission of the flooded site ranges from 98 to 171 g C m⁻²yr⁻¹. There is no diurnal pattern observed for the flooded site in general. But there is a strong seasonal pattern of CO₂ emission with two major emission peaks takes place. The first and most intensive peak happens in early May corresponding to the ice break up, and the second peak usually occurs in late August and early September, corresponding to the autumn reservoir turnover. For all of the time, the flooded site is a carbon emitter with a positive CO₂ flux.

The net effect of flooding a boreal forest to create a hydroelectric reservoir is an increase in the carbon emission. The net carbon emission after flooding ranges from 181 g C m⁻²yr⁻¹ to 242 g C m⁻²yr⁻¹. The impoundment turns the boreal ecosystem from a carbon sink to a carbon source, offsetting the carbon that was originally being fixed by forest and

adding more CO₂ to the atmosphere annually.

In the current study, the Eastmain-1-A powerhouse has an annual power output of 2.3 TWh (Hydro Quebec, n.d.) and an annual carbon emission of 173 to 232 g CO₂ yr⁻¹ kWh⁻¹. In comparison, a natural-gas-based electricity generator emits 419 g CO₂ yr⁻¹ kWh⁻¹ and a coal-based electricity generator emits 1001 g CO₂ yr⁻¹ kWh⁻¹ (U.S. EIA, n.d.). Therefore, although the creation of hydroelectric reservoir results in extra carbon emission to the atmosphere, hydroelectricity production still emits less CO₂ than conventional fossil-fuel-based electricity generators.

REFERENCE LIST

- Baldocchi, D. D. (2003). Assessing the eddy covariance technique for evaluating carbon dioxide exchange rates of ecosystems: past, present and future. *Global Change Biology*, 9(4), 479–492. doi: 10.1046/j.1365-2486.2003.00629.x
- Bergeron, O., Margolis, H. A., Black, T. A., Coursolle, C., Dunn, A. L., Barr, A. G., & Wofsy, S. C. (2007). Comparison of carbon dioxide fluxes over three boreal black spruce forests in Canada. *Global Change Biology*, 13(1), 89–107. doi: 10.1111/j.1365-2486.2006.01281.x
- Chao, B. F. (1994). Man-made lakes and sea-level rise. *Nature*, 370(6487), 258–258. doi: 10.1038/370258a0
- Chao, B. F. (1995). Anthropogenic impact on global geodynamics due to reservoir water impoundment. *Geophysical Research Letters*, 22(24), 3529–3532. doi: 10.1029/95gl02664
- Duchemin, E., Lucotte, M., Canuel, R., & Chamberland, A. (1995). Production of the greenhouse gases CH₄ and CO₂ by hydroelectric reservoirs of the boreal region. *Global Biogeochemical Cycles*, 9(4), 529–540. doi: 10.1029/95gb02202
- Duchemin, E., Lucotte, M., Canuel, R., Queiroz, A. G., Almeida, D. C., Pereira, H. C., & Dezincourt, J. (2000). Comparison of greenhouse gas emissions from an old tropical reservoir with those from other reservoirs worldwide. *SIL Proceedings, 1922-2010*, 27(3), 1391–1395. doi: 10.1080/03680770.1998.11901464
- Dunn, A. L., Barford, C. C., Wofsy, S. C., Goulden, M. L., & Daube, B. C. (2007). A long-term record of carbon exchange in a boreal black spruce forest: means, responses to interannual variability, and decadal trends. *Global Change Biology*, 13(3), 577–590. doi: 10.1111/j.1365-2486.2006.01221.x
- Dunn, A. L., Wofsy, S. C., & Bright, A. H. (2009). Landscape heterogeneity, soil climate, and carbon exchange in a boreal black spruce forest. *Ecological Applications*, 19(2), 495–504. doi: 10.1890/07-0771.1
- Falge, E., Baldocchi, D., Olson, R., Anthoni, P., Aubinet, M., Bernhofer, C., ... Wofsy, S. (2001). Gap filling strategies for defensible annual sums of net ecosystem exchange. *Agricultural and Forest Meteorology*, 107(1), 43–69. doi: 10.1016/s0168-1923(00)00225-2
- Goulden, M. L., Winston, G. C., Mcmillan, A. M. S., Litvak, M. E., Read, E. L., Rocha, A. V., & Elliot, J. R. (2006). An eddy covariance mesonet to measure the effect of forest age on land-atmosphere exchange. *Global Change Biology*, 12(11), 2146–2162. doi: 10.1111/j.1365-2486.2006.01251.x

- Granier, A., Ceschia, E., Damesin, C., Dufrene, E., Epron, D., Gross, P., ... Saugier, B. (2000). The carbon balance of a young Beech forest. *Functional Ecology*, *14*(3), 312–325. doi: 10.1046/j.1365-2435.2000.00434.x
- Hydroquebec (n.d.). Retrieved from <http://www.hydroquebec.com/sebj/en/eastmain-1-a-sarcelle-rupert.html>
- Iremonger, S., Ravilious, C., & Quinton, T. (Eds.). (1997). A global overview of forest conservation. World Conservation Monitoring Centre.
- Jackson, S., & Sleight, A. (2000). Resettlement for Chinas Three Gorges Dam: socio-economic impact and institutional tensions. *Communist and Post-Communist Studies*, *33*(2), 223–241. doi: 10.1016/s0967-067x(00)00005-2
- Kelly, C. A., Rudd, J. W. M., Louis, V. L. S., & Moore, T. (1994). Turning attention to reservoir surfaces, a neglected area in greenhouse studies. *Eos, Transactions American Geophysical Union*, *75*(29), 332. doi: 10.1029/94eo00987
- Kim, Y., Roulet, N. T., Li, C., Frohling, S., Strachan, I. B., Peng, C., ... Tremblay, A. (2016). Simulating carbon dioxide exchange in boreal ecosystems flooded by reservoirs. *Ecological Modelling*, *327*, 1–17. doi: 10.1016/j.ecolmodel.2016.01.006
- Lasslop, G., Reichstein, M., Papale, D., Richardson, A. D., Arneeth, A., Barr, A., ... Wohlfahrt, G. (2010). Separation of net ecosystem exchange into assimilation and respiration using a light response curve approach: critical issues and global evaluation. *Global Change Biology*, *16*(1), 187–208. doi: 10.1111/j.1365-2486.2009.02041.x
- Law, B., Baldocchi, D., & Anthoni, P. (1999a). Below-canopy and soil CO₂ fluxes in a ponderosa pine forest. *Agricultural and Forest Meteorology*, *94*(3-4), 171–188. doi: 10.1016/s0168-1923(99)00019-2
- Law, B. E., Ryan, M. G., & Anthoni, P. M. (1999b). Seasonal and annual respiration of a ponderosa pine ecosystem. *Global Change Biology*, *5*(2), 169–182. doi: 10.1046/j.1365-2486.1999.00214.x
- Lehner, B., Liermann, C. R., Revenga, C., Vörösmarty, C., Fekete, B., Crouzet, P., ... Wisser, D. (2011). High-resolution mapping of the worlds reservoirs and dams for sustainable river-flow management. *Frontiers in Ecology and the Environment*, *9*(9), 494–502. doi: 10.1890/100125
- Lemieux, M. (2010). *From Forest to Lake: Effect of Hydroelectric Reservoir Impoundment on the Net Ecosystem Exchange of CO₂* (Unpublished master's thesis). McGill University, Montreal, Quebec, Canada.
- Livingston, G.P. & Hutchinson, G.L.. (1995). Enclosure-based measurement of trace gas exchange: application and sources of error. *Biogenic Trace Gases: Measuring*

Emissions from Soil and Water. 14-50.

- Louis, V. L. S., Kelly, C. A., Duchemin, É., Rudd, J. W. M., & Rosenberg, D. M. (2000). Reservoir Surfaces as Sources of Greenhouse Gases to the Atmosphere: A Global Estimate. *BioScience*, *50*(9), 766. doi: 10.1641/0006-3568(2000)050[0766:rsasog]2.0.co;2
- McMillan, A. M. S., Winston, G. C., & Goulden, M. L. (2008). Age-dependent response of boreal forest to temperature and rainfall variability. *Global Change Biology*, *14*(8), 1904–1916. doi: 10.1111/j.1365-2486.2008.01614.x
- Payeur-Poirier, J.-L., Coursolle, C., Margolis, H. A., & Giasson, M.-A. (2012). CO₂ fluxes of a boreal black spruce chronosequence in eastern North America. *Agricultural and Forest Meteorology*, *153*, 94–105. doi: 10.1016/j.agrformet.2011.07.009
- Podgrajsek, E., Sahlée, E., Bastviken, D., Holst, J., Lindroth, A., Tranvik, L., & Rutgersson, A. (2014). Comparison of floating chamber and eddy covariance measurements of lake greenhouse gas fluxes. *Biogeosciences*, *11*(15), 4225–4233. doi: 10.5194/bg-11-4225-2014
- Reichstein, M., Falge, E., Baldocchi, D., Papale, D., Aubinet, M., Berbigier, P., ... Valentini, R. (2005). On the separation of net ecosystem exchange into assimilation and ecosystem respiration: review and improved algorithm. *Global Change Biology*, *11*(9), 1424–1439. doi: 10.1111/j.1365-2486.2005.001002.x
- Rosenberg, D. M., Berkes, F., Bodaly, R. A., Hecky, R. E., Kelly, C. A., & Rudd, J. W. (1997). Large-scale impacts of hydroelectric development. *Environmental Reviews*, *5*(1), 27–54. doi: 10.1139/a97-001
- Schlesinger, W. H., & Bernhardt, E. S. (2013). *Biogeochemistry: an analysis of global change*. Amsterdam: Elsevier.
- Soloway, A. D., Amiro, B. D., Dunn, A. L., & Wofsy, S. C. (2017). Carbon neutral or a sink? Uncertainty caused by gap-filling long-term flux measurements for an old-growth boreal black spruce forest. *Agricultural and Forest Meteorology*, *233*, 110–121. doi: 10.1016/j.agrformet.2016.11.005
- Strachan, I. B., Pelletier, L., & Bonneville, M.-C. (2015). Inter-annual variability in water table depth controls net ecosystem carbon dioxide exchange in a boreal bog. *Biogeochemistry*, *127*(1), 99–111. doi: 10.1007/s10533-015-0170-8
- Strachan, I. B., Tremblay, A., Pelletier, L., Tardif, S., Turpin, C., & Nugent, K. A. (2016). Does the creation of a boreal hydroelectric reservoir result in a net change in evaporation? *Journal of Hydrology*, *540*, 886–899. doi: 10.1016/j.jhydrol.2016.06.067
- Tadonlélé, R. D., Marty, J., & Planas, D. (2011). Assessing factors underlying variation of

CO₂ emissions in boreal lakes vs. reservoirs. *FEMS Microbiology Ecology*, 79(2), 282–297. doi: 10.1111/j.1574-6941.2011.01218.x

Teodoru, C. R., Bastien, J., Bonneville, M.-C., Giorgio, P. A. D., Demarty, M., Garneau, M., ... Tremblay, A. (2012). The net carbon footprint of a newly created boreal hydroelectric reservoir. *Global Biogeochemical Cycles*, 26(2). doi: 10.1029/2011gb004187

Tremblay, A., Lambert, M., & Gagnon, L. (2004). Do Hydroelectric Reservoirs Emit Greenhouse Gases? *Environmental Management*, 33(S1). doi: 10.1007/s00267-003-9158-6

Tremblay, A., Tardif, S., & Strachan, I. B. (2020, April 6). Studying Net Evaporation from the Eastmain-1 Reservoir. Retrieved from <https://www.renewableenergyworld.com/2014/06/18/studying-net-evaporation-from-the-eastmain-1-reservoir/#gref>

U.S. Energy Information Administration - EIA - Independent Statistics and Analysis. (n.d.). Retrieved from <https://www.eia.gov/tools/faqs/faq.php?id=74&t=11>

Umehara, A., Komorita, T., Takahashi, T., & Tsutsumi, H. (2019). Estimation of production and sedimentation of cyanobacterial toxins (microcystin) based on nutrient budgets in the reservoir of Isahaya Bay, Japan. *Ecotoxicology and Environmental Safety*, 183, 109477. doi: 10.1016/j.ecoenv.2019.109477

Wind Rose - File Exchange - MATLAB Central. (n.d.). Retrieved from <https://www.mathworks.com/matlabcentral/fileexchange/47248-wind-rose>

Wilmsen, B., Webber, M., & Duan, Y. (2011). Involuntary Rural Resettlement. *The Journal of Environment & Development*, 20(4), 355–380. doi: 10.1177/1070496511426478

Xu, Z., Yin, X., Sun, T., Cai, Y., Ding, Y., Yang, W., & Yang, Z. (2017). Labyrinths in large reservoirs: An invisible barrier to fish migration and the solution through reservoir operation. *Water Resources Research*, 53(1), 817–831. doi: 10.1002/2016wr019485

APPENDIX

The thesis analyzed the data in Chapter 4 using the octave scripts created by author, which can be accessed via: <https://github.com/WilliamTianqiXing/undergraduate-honour.git>

Source code of wind rose figures function by Daniel Pereira (modified by author) can be accessed via: <https://www.mathworks.com/matlabcentral/fileexchange/47248-wind-rose>